International Journal of Nanomedicine

Dovepress
Taylor & Francis Group

Open Access Full Text Article

REVIEW

Deep Tumor Penetration Using Nanoparticle Delivery Systems: Programmed Design Strategies and Emerging Evaluation Platforms

Mahsa Javan[1,2], Deniz Ajabi Zareian[1,3], Solmaz Mojarad-Jabali[4]

[1]Tabriz University of Medical Sciences, Tabriz, Iran; [2]Department of Medicinal Chemistry, Faculty of Pharmacy, Tabriz University of Medical Sciences, Tabriz, Iran; [3]Pharmaceutical Biotechnology Research Center, Zanjan University of Medical Sciences, Zanjan, Iran; [4]Pharmaceutical Sciences Research Center, Mazandaran University of Medical Sciences, Sari, Iran

Correspondence: Solmaz Mojarad-Jabali, Pharmaceutical Sciences Research Center, Mazandaran University of Medical Sciences, PO Box- 48175/861, Sari, Iran, Tel +98 11 33543081-3, Fax +98 11 33543084, Email s.mojarad3973@gmail.com

Abstract: The complex architecture of solid tumors, including dense extracellular matrix and abnormal vasculature, impedes effective nanoparticle (NP) delivery. Conventional NPs often fail to penetrate deeply due to their fixed size, rapid clearance, and poor tumor retention. Unlike previous reviews that focus solely on physicochemical properties, this article critically evaluates "programmed" delivery strategies that dynamically adapt to physiological barriers. Size-transformable nanocarriers offer a promising solution by remaining large during circulation to exploit the enhanced permeability and retention (EPR) effect, then shrinking in response to tumor-specific stimuli (eg, low pH, high glutathione, or enzymatic activity), thereby improving tumor penetration and drug release This review highlights recent advances in overcoming these obstacles, with a focus on programmed delivery strategies NPs with a size-switching technique degrade upon reaching the tumor site, allowing for deeper penetration. Surface modification enhances interactions with the tumor microenvironment (TME), whereas ligands improve target selectivity and tumor cell uptake, and altering the NP form improves their delivery and distribution within tumors. Uniquely, the review bridges the gap between design and evaluation by discussing emerging experimental platforms such as 3D tumor models and microfluidic chips. Finally, it examines the growing role of artificial intelligence (AI) and in silico modeling in optimizing NP design, offering insights into precision nanomedicine.

Keywords: nanoparticle, tumor penetration, drug delivery, tumor microenvironment, smart systems

Introduction

Tumors are complex and highly heterogeneous masses characterized by rapid cell proliferation, abnormal microenvironments, and specialized structural components, such as the extracellular matrix (ECM) and stromal cells, that protect cancer cells and support their survival.[1] The tumor microenvironment (TME), particularly in solid tumors, presents significant barriers to effective drug delivery due to its abnormal architecture and composition.[2,3] Elevated interstitial fluid pressure (IFP), dense stromal populations, and a rigid ECM collectively hinder the transport of therapeutic agents, including nanoparticles (NPs), thereby compromising treatment efficacy.[4,5] High IFP forms a physical barrier that limits NP penetration and contributes to heterogeneous intratumoral drug distribution.[6,7] Additionally, stromal cells not only hinder NP movement but also support cancer cell survival through structural and signaling mechanisms.[8,9] The dense ECM further restricts NP diffusion, limiting their accumulation in deeper tumor regions such as the hypoxic core.[10] Beyond these physical impediments, the heterogeneous and aberrant vascular architecture of tumors, often structurally irregular and regionally insufficient, further compromises NP delivery, leading to limited therapeutic distribution within the tumor core and hypoxic zones.[11,12]

Despite the numerous physical and biological impediments posed by the TME, recent research has primarily focused on optimizing the physicochemical properties of NPs, such as surface characteristics, morphology, and size, to enhance

https://doi.org/10.2147/IJN.S563233
Received: 26 August 2025
Accepted: 21 March 2026
Published: 14 April 2026

Graphical Abstract

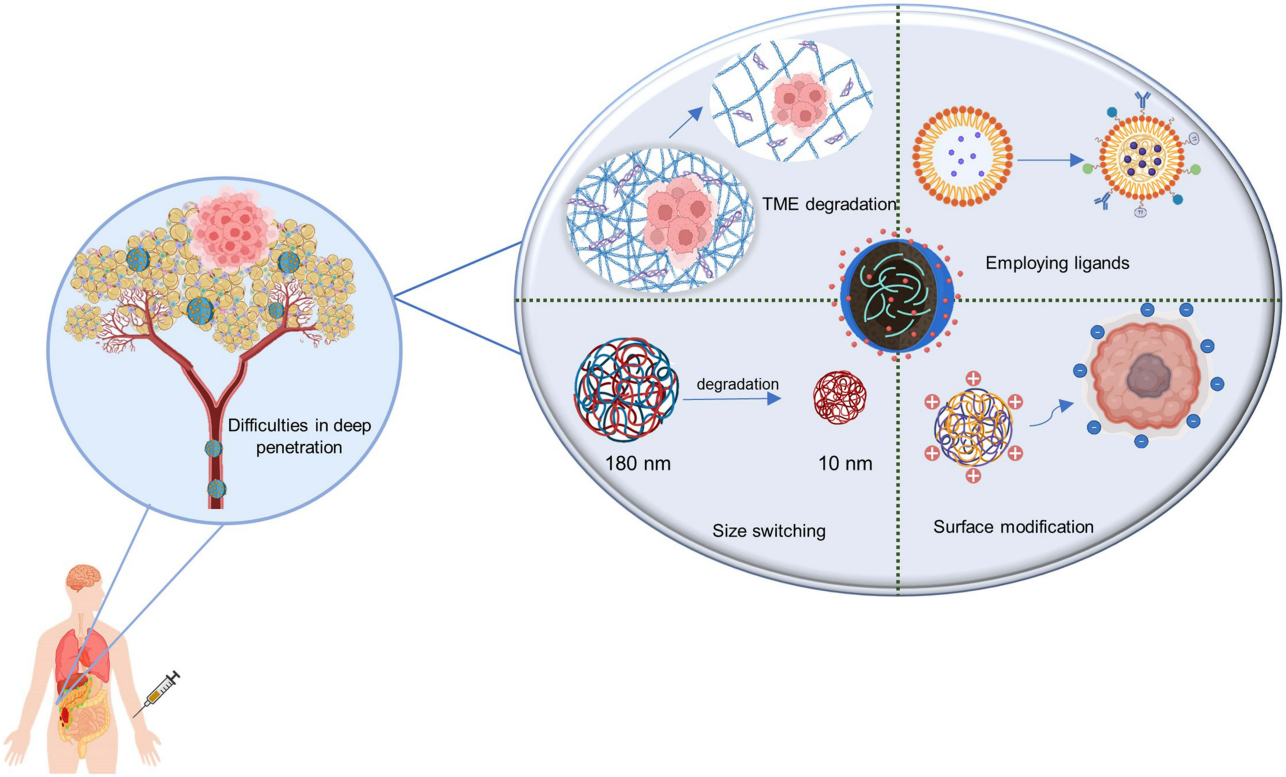

their intratumoral penetration and therapeutic efficacy.[13,14] Optimizing particle size can facilitate movement through the dense ECM, thereby improving access to poorly perfused and deeper tumor regions.[15,16] Additionally, modifying NP shape has been shown to affect cellular uptake and facilitate their passage through the TME.[17,18] Surface modifications, including polyethylene glycol (PEG) PEGylation and the conjugation of targeting ligands, can prolong systemic circulation, reduce immunogenic clearance, and increase tumor-specific accumulation.[19] Generally, these design strategies contribute to more efficient and targeted drug delivery, enhancing both NP penetration and retention within tumor tissues while minimizing off-target effects.[4]

Beyond structural optimization, innovative delivery strategies have been developed to enhance NP penetration into tumors further.[20] For instance, size-switching NPs, which are engineered to alter their size in response to stimuli within the TME, have shown improved penetration into deeper tumor layers.[21] Additionally, functionalizing NP surfaces with ligands targeting specific receptors on tumor cells or ECM components can enhance localization and binding, thereby improving delivery efficiency.[22] Surface charge modulation represents another promising approach, enabling NPs to adapt to dynamic physicochemical conditions within tumors, ultimately enhancing their transport and retention in the TME.[23]

Complementing these experimental strategies, in silico approaches are increasingly being integrated into NP design and delivery optimization.[24] Computational modeling and simulations facilitate the prediction of NP behavior under various physiological and physicochemical conditions, enabling the assessment of delivery outcomes before in vivo experimentation.[25–27] These tools significantly reduce the trial-and-error burden in experimental workflows and contribute to the rational design of NPs with improved therapeutic efficacy and tumor penetration.[28]

In this review, the significant physiological and structural barriers to deep NP penetration in solid tumors, including the Blood-Brain Barrier (BBB), dense ECM, elevated IFP, heterogeneous vascular networks, and abundant stromal cells,

are highlighted. Programmed delivery strategies, such as size-switching systems, surface functionalization, and ligand-mediated targeting, as well as biomimetic cellular hitchhiking (eg, Trojan horse strategies), are then discussed Furthermore, emerging experimental platforms, including spheroids, organoids, and microfluidic tumor-on-a-chip systems, are evaluated as critical tools for mimicking the complex TME Finally, the integration of in silico modeling as a complementary strategy is highlighted as a framework to complement experimental approaches, enabling the prediction of NP behavior and the optimization of delivery parameters under physiologically relevant conditions Collectively, these experimental and computational advancements offer a comprehensive approach to overcoming intratumor delivery barriers and improving the efficacy of NP-based cancer therapies.

Biophysical and Cellular Barriers Limiting Deep Penetration of Nanoparticles into Solid Tumors

Efficient and deep penetration of NPs into solid tumors is hindered by a set of barriers within the TME, including elevated IFP, a dense ECM, stromal cells, and heterogeneous vasculature (Figure 1).[29–32] These structural and physiological features, combined with thick, heterogeneous tumor cells and abundant stromal components, significantly compromise the efficacy of NP-based therapies.[33,34] Therefore, understanding and addressing these multifaceted barriers is essential to enhance the therapeutic potential of nanomedicine in oncology.[35]

Interstitial Fluid Pressure (IFP)

IFP is a critical component of the TME that significantly influences the distribution and therapeutic effectiveness of NPs in cancer treatment.[36] Elevated IFP results from abnormal vascular structures, lymphatic dysfunction, and rapid tumor growth, which together disrupt fluid dynamics within tumors and impede the penetration and retention of NPs.[37] This

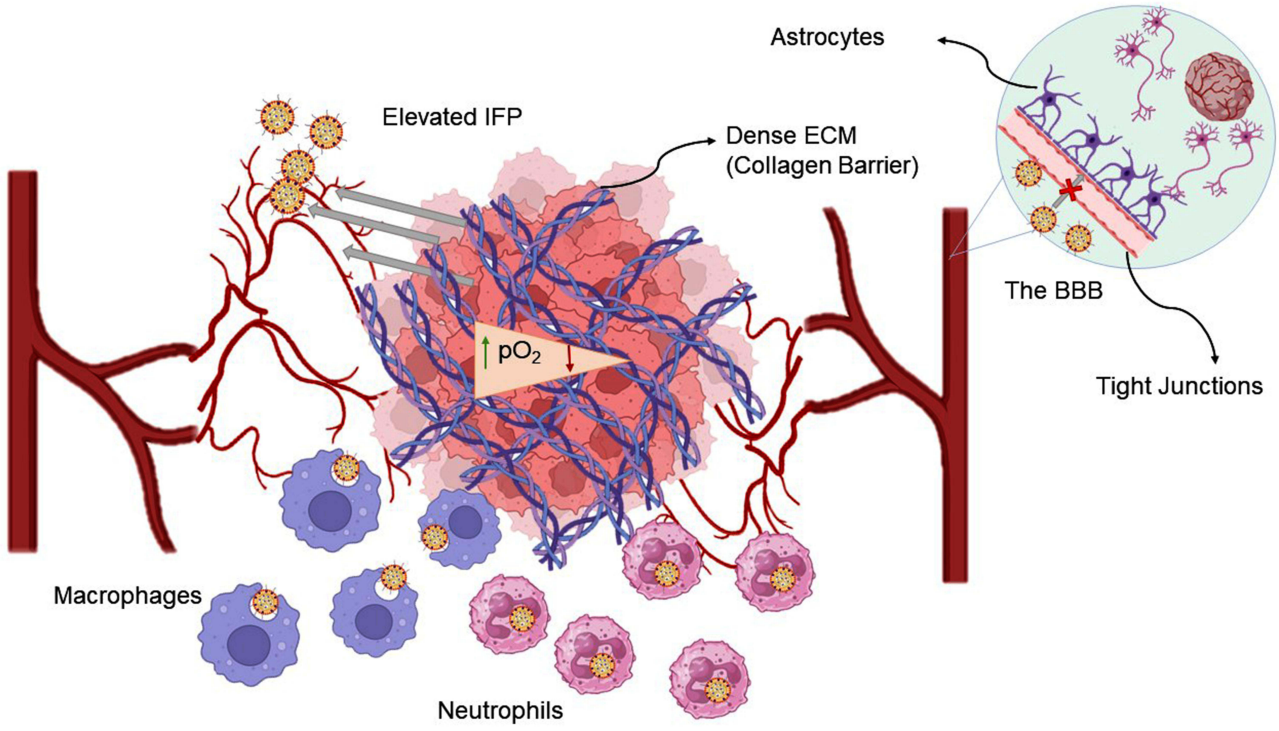

Figure 1 Schematic illustration of the major biophysical and cellular barriers in the tumor microenvironment (TME) restricting nanoparticle penetration. The diagram highlights critical impediments, including elevated interstitial fluid pressure (IFP), dense extracellular matrix (ECM) composed of collagen fibers, and hypoxic regions (low pO_2), arrows denote the oxygen gradient (pO_2), with ↑ indicating higher oxygen levels and ↓ indicating hypoxia toward the tumor core. It also illustrates the distinct physiological barrier of the Blood-Brain Barrier (BBB) characterized by tight junctions and astrocytes, alongside the immunosuppressive immune landscape populated by tumor-associated macrophages and neutrophils. The red cross symbol denotes restricted or failed nanoparticle transport due to the tumor-associated biophysical barriers.

https://doi.org/10.2147/IJN.S563233

elevated pressure promotes the efflux of NPs from the tumor interstitial space back into the tumor vasculature, thereby reducing intratumoral accumulation and compromising therapeutic efficacy.[38]

To address the effects of IFP, Yu et al investigated the use of cediranib, a vascular endothelial growth factor receptor (VEGFR) inhibitor known to normalize tumor vasculature and modulate the TME. In their study, pretreatment with cediranib markedly enhanced the intratumoral accumulation of gold NPs in solid tumors.[21] Cediranib functions as a competitive inhibitor of all three VEGFR isoforms, thereby suppressing angiogenesis and contributing to the reduction of IFP.[39] While vascular normalization aims to lower IFP, an alternative strategy is to enable NPs to traverse biological barriers despite elevated IFP. To address this, Wang et al demonstrated that transcytosis of a dendrimer-camptothecin (CPT) conjugate, mediated by γ-glutamyl transpeptidase (GGT), is an effective strategy for treating pancreatic ductal adenocarcinoma (PDAC). Their innovative approach involved designing dendrimer structures with tailored surface chemistry, which not only enhanced transcytosis but also enabled deeper penetration into PDAC, characterized by a dense ECM and elevated IFP. This strategy not only improves drug delivery but also addresses the barriers imposed by the TME, ultimately contributing to more effective therapeutic outcomes.[40]

Dense Extracellular Matrix (ECM)

A major contributor to poor prognosis in many solid tumors is the extensive development of a dense fibrotic stroma, characterized by excessive deposition of ECM components, including collagen, elastin, and glycoproteins.[41] High ECM density contributes to increased tumor stiffness and elevated IFP.[42] This dense matrix generates substantial mechanical stress, which restricts the penetration of therapeutic agents, particularly larger molecules such as drug-loaded nanocarriers, into tumor tissues.[37]

Collagen, the predominant structural protein in the ECM, plays a key role in establishing a fibrotic microenvironment that severely hinders the effective delivery of chemotherapeutic agents and nanomedicines.[43] Consequently, collagenase has been widely investigated as an ECM-degrading enzyme to improve drug delivery.[44] However, systemic administration of collagenase raises safety concerns, as elevated circulating levels can degrade typical tissue structures.[45] To overcome this, Yang et al developed a nanoplatform using gold nanocages functionalized with collagenase to degrade the ECM in PDAC locally (Figure 2).[46] The platform employed biomimetic cell membrane coating and lipid insertion techniques to anchor collagenase to the NP surface. Results demonstrated that doxorubicin (DOX)-loaded gold nanocages (Col-M@AuNCs/Dox) significantly reduced collagen content within the tumor ECM, thereby enhancing drug penetration into PDAC tissues.

In addition to enzymatic degradation, nitric oxide (NO) has been shown to facilitate ECM remodeling. NO interacts with superoxide anions in the TME to form peroxynitrite, an oxidant that activates matrix metalloproteinases (MMPs).[47,48] These MMPs degrade collagen and other ECM components, improving NP diffusion.[49] For this purpose, Wan et al developed heparin/folic acid/L-arginine (HFLA) NPs that function as both anticancer agents and targeting moieties for cancer cells. These NPs serve as carriers for the chemotherapy drug DOX, forming HFLA-DOX nanomotors. Given the higher levels of NO synthase and reactive oxygen species (ROS) present in tumor environments compared to normal tissues, HFLA nanomotors can generate NO, which powers the nanomotors and facilitates their intracellular distribution and intercellular transit.[50] Expanding on this NO-driven strategy for immunotherapy, Chen et al created a NO-driven nanomotor based on heparin/folate-Cy5.5/L-arginine, co-encapsulating docetaxel, and the immune checkpoint inhibitor anti-programmed cell death protein 1 (anti-PD-1). Their study reported a 13-fold increase in T cell infiltration when using this system, compared to conventional delivery methods.[51]

An alternative, non-chemical approach involves high-intensity focused ultrasound (HIFU), which can locally disrupt the ECM with minimal toxicity to adjacent normal tissues.[52,53] Choi et al applied HIFU at specific parameters (5 W/cm^2 intensity, 1.5 MHz frequency, 10% duty cycle, 1 Hz repetition, 30s per spot), effectively degrading ECM barriers and enhancing the penetration of DOX-loaded glycol chitosan NPs in A549 tumor-bearing mice.[54]

Another major ECM component is hyaluronic acid (HA), which forms a hydrated gel-like matrix that supports tumor growth and contributes to poor drug penetration.[55] Hyaluronidase is an enzyme that hydrolyzes HA, leading to ECM degradation and subsequent modulation of the TME, including improved vascular function and reduced hypoxia.[56,57] Yang et al developed HPR@CCP NPs, featuring a HA shell for CD44-mediated targeting and a core containing

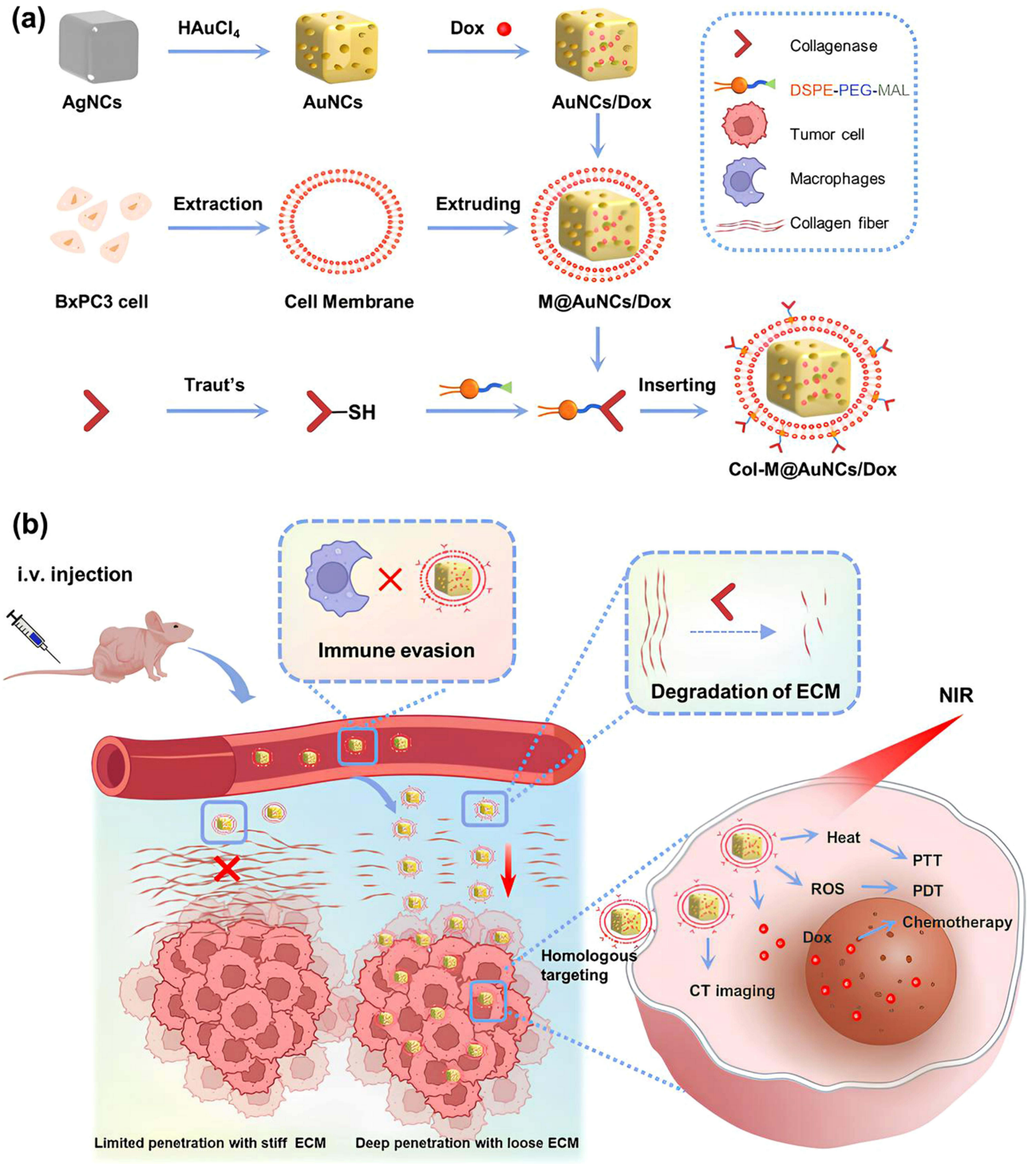

Figure 2 Schematic illustration of (**a**) the preparation of Col-M@AuNCs/Dox. The blue arrows indicate the sequential steps of synthesis, membrane coating, and modification. (**b**) The mechanism of action combining ECM degradation and chemotherapy. The red cross symbol (**X**) near macrophages indicates the inhibition of macrophage uptake, representing immune evasion. The red cross symbol (**X**) within the dense extracellular matrix denotes restricted nanoparticle penetration in stiff ECM. The red downward arrow (↓) represents enhanced inward transport and deep penetration of nanoparticles into tumor tissue following ECM degradation. Inside the cancer cell, arrows depict the pathways for photothermal therapy (PTT), photodynamic therapy (PDT), and chemotherapy. Adapted with permission from.[46]

a CRISPR-Cas9 system targeting the Ptpn2 gene (Cas9-Ptpn2), along with a mitochondria-targeting chlorin e6 (Ce6) derivative containing triphenylphosphonium (TPP) and polyethylenimine (PEI) (TPP-PEI-Ce). This system was designed to enhance therapeutic efficacy against both primary tumors and distant metastases. Pre-treatment with hyaluronidase not

https://doi.org/10.2147/IJN.S563233

only degraded the HA shell (reducing NP size and facilitating deeper tumor penetration) but also improved the ECM structure, regulated tumor vasculature, and alleviated hypoxia, collectively contributing to enhanced therapeutic outcomes.[58] In contrast to strategies focused on ECM degradation, an alternative approach is to bypass the dense barrier entirely. Exploring this concept, Wang et al designed GSHPTCPT NPs by conjugating CPT to Poly(amidoamine) (PAMAM) dendrimers via a ROS-sensitive thioketal linker and modifying the surface with glutathione (GSH) to create a GGT-responsive delivery system. This design enabled tumor-specific charge reversal upon exposure to GGT, thereby triggering caveolae-mediated endocytosis and transcytosis, facilitating deep tumor penetration. Rather than enzymatically degrading the ECM, this system bypassed dense stromal barriers through GGT-triggered cationization and transcellular transport, allowing efficient intratumoral drug distribution.[40]

Another strategy to reduce the ECM involves enzymatic digestion using thermostable enzymes, such as proteases and glycosidases, that retain high activity at higher temperatures.[59] To address the limited stability of conventional enzymes in the complex TME, Wu et al employed papain, a temperature-responsive protease with broad substrate specificity and high stability, to selectively degrade the ECM under near-infrared II (NIR-II) light stimulation within a nanosystem composed of a gold nanorod core and a PEGylated mesoporous polydopamine (mPDA) shell. This shell protected the enzyme until activation by NIR-II light, enabling localized ECM degradation and enhanced delivery of therapeutic agents.[60]

Stromal Cells

The mesodermal germ layer gives rise to mesenchymal stromal cells (MSCs), which are multipotent cells capable of differentiating into skeletal muscle, connective tissue, and vascular cell types.[61–63] These cells play essential roles in maintaining tissue structure and regulating a wide range of physiological processes.[64] In the context of cancer, stromal cells are critical components of the TME. The TME comprises various stromal cell populations, including mesenchymal stem cells, cancer-associated fibroblasts (CAFs), tumor-associated macrophages (TAMs), lymphocytes, endothelial cells, and pericytes. These cells actively support tumor progression by influencing metabolic pathways, promoting tumor growth and metastasis, facilitating immune evasion, and contributing to therapy resistance.[65,66] Understanding the cellular composition of the TME and distinguishing stromal cells from tumor cells is essential for designing effective targeted therapies. To achieve this, Li et al established a subcutaneous xenograft model by injecting BxPC-3 pancreatic cancer cells labeled with green fluorescent protein (GFP) into nude mice. In heterogeneous tumor tissue, GFP labeling enabled visual differentiation of tumor cells from surrounding stromal cells. The GFP-positive tumor cells were isolated by fluorescence-activated cell sorting (FACS) after treatment with drug-loaded NPs, and their drug accumulation was evaluated separately. This approach provided a more precise determination of how treatment affects the tumor cells specifically.[67]

Once identified, it becomes evident that specific stromal subtypes act as major sinks for nanotherapeutics. Among these populations, CAFs and TAMs are particularly prominent because of their significant roles at all stages of tumor development. These cells interact closely with cancer cells to promote proliferation, invasion, and resistance to therapy.[65,68] CAFs, in particular, secrete growth factors, cytokines, and MMPs that drive angiogenesis, ECM remodeling, and metastasis.[69] Importantly, both CAFs and TAMs also influence the fate of nanomedicine within tumors. Their presence affects the distribution, retention, and release of NPs in the TME.[70] For instance, CAFs, which are often located near tumor vasculature, exhibit high NP uptake, especially for particles smaller than 100 nm, thereby enhancing accumulation through the EPR effect.[71] Providing quantitative evidence of this barrier effect, a study reported that CAFs internalized NPs at rates seven times higher than tumor cells 16 hours post-injection, while TAMs captured over 40% of injected polymeric NPs.[72]

Heterogeneous Vascular Network

In addition to ECM barriers, the abnormal and heterogeneous vascular structure within solid tumors significantly limits the ability of NPs to reach cancer cells—particularly those located in the tumor core.[73,74] This compromised vasculature is a key factor in the limited efficacy observed with many clinically approved nanomedicines, as it impedes deep tumor penetration.[75,76] The rapid proliferation of tumor cells leads to the formation of leaky, disorganized, and tortuous blood vessels.[77] Simultaneously, the overexpression of angiogenic factors results in a heterogeneous vascular network that lacks the uniformity and structural integrity found in normal tissues.[78] These abnormalities contribute to elevated IFP and reduced perfusion, further obstructing the intratumoral transport of therapeutic agents.[79]

One promising therapeutic strategy is vascular normalization, which aims to remodel abnormal tumor vessels by decreasing vascular leakage, improving vessel structure, and restoring functional perfusion. These changes enhance the delivery of anticancer drugs to tumor cells, reduce IFP, and facilitate deeper penetration of therapeutic agents into the tumor tissue.[80] In a notable study, Tong et al demonstrated that blocking VEGFR-2 with the monoclonal antibody (mAb) DC101 led to normalization of the tumor vasculature. This intervention reduced vessel diameter and tortuosity while increasing pericyte and basement membrane coverage, resulting in a more stable and organized vascular network. The normalized vessels were associated with reduced IFP, enhanced oncotic pressure gradients across the tumor vasculature, and improved delivery of large therapeutic agents and large molecules (such as bovine serum albumin (BSA)) to the tumor site.[81]

Although abnormal tumor vasculature may initially facilitate NP extravasation, it also elevates IFP, which can drive NPs out of the tumor tissue and back into the bloodstream. This effect leads to poor distribution within the tumor core and significantly compromises therapeutic efficacy.[79] Building on the effectiveness of VEGFR inhibition strategies, Yu et al pretreated tumors with cediranib, a VEGFR inhibitor known to normalize tumor vasculature. This approach enhanced the accumulation of gold NPs within tumors and modified the TME, improving overall antitumor efficacy.[21]

Vascular normalization also plays a critical role in immune modulation, particularly in supporting T cell infiltration.[82] Beyond enhancing drug accumulation, vascular normalization is pivotal for overcoming immune exclusion. To illustrate this immunomodulatory effect, Chen et al showed that NO-releasing nanomotors facilitated normalization of the tumor vasculature, thereby significantly enhancing T-cell infiltration and transport. Treatment with nanomotors decreased mean vascular density and increased the number of perfused functional blood vessels, resulting in improved oxygenation and vascular function within the tumor, facilitating more efficient delivery of drugs and immune cells.[51] While normalization aims to repair vessel structure, an alternative approach involves engineering nanoparticles that adapt to the disordered vascular constraints. For instance, Lin et al developed a GSH-responsive, size-transformable Janus NP system (JNP Ve) to overcome both the dense ECM and aberrant tumor vasculature. These NPs disassemble in response to the high GSH concentrations typically found in the TME, breaking down into smaller components, such as gold NPs, manganese ions (Mn^{2+}), and NIR dyes, that demonstrate superior tissue penetration compared to their larger precursors.[74]

Tumor Immune Microenvironment

A characteristic of cancer is genetic instability, which leads to the production of abnormal proteins unfamiliar to the immune system. The host immune system can inherently eradicate malignant cells through the cancer-immunity cycle; nevertheless, tumors develop strategies to transform this environment into an immunosuppressive state, thereby escaping detection and facilitating tumor development.[83] In TME, numerous innate immune cells indirectly affect tumor growth by regulating T-cell activities.[84,85] Innate immune cells, including TAMs, neutrophils, dendritic cells, natural killer (NK) cells, and myeloid-derived suppressor cells (MDSCs), shape the inflammatory environment through phagocytosis, cytokine secretion, and immunosuppressive mechanisms that directly influence NP distribution and immune activation.[86,87] A summary of these bio-inspired strategies, including cellular hitchhiking and membrane-coating approaches using macrophages, neutrophils, and dendritic cells, is provided in Table 1.

Macrophages

Macrophages, known for their diversity and multifunctionality, play key roles in various physiological processes, such as sustaining tissue homeostasis, regulating tumor progression, and protecting the body from infections.[96] Polarized macrophages are divided into two main subtypes, M1 and M2, both of which are closely involved in tumor immunity.[97] Classically activated M1 macrophages, which serve as primary mediators of the proinflammatory response, undergo polarization when exposed to stimuli such as lipopolysaccharide (LPS), interferon-γ (IFN-γ), granulocyte-macrophage colony-stimulating factor (GM-CSF), or various pathogen-associated molecular patterns (PAMPs).[96,98] Following activation, these macrophages synthesize and secrete key proinflammatory cytokines, including interleukin-6 (IL-6), IL-12, and tumor necrosis factor (TNF). Beyond cytokine production, they exhibit direct anti-tumorigenic properties by identifying and phagocytosing neoplastic cells, thereby suppressing tumor proliferation and metastatic dissemination. Additionally, they function as effective antigen-presenting cells (APCs), priming T lymphocytes to elicit targeted adaptive immune responses.[96,99] In contrast to the proinflammatory M1 phenotype, alternatively activated M2

Table 1 Bio-Inspired "Trojan Horse" Cellular Hitchhiking and Membrane-Coating Strategies

Carrier Cell	Strategy	Ligand/ Receptor	Mechanism	Payload	In vivo Model/Tumor Type	Key Findings	Ref.
Macrophage	Backpacking "DMPM"	MCP-1 peptide targeting CCR2 receptor	pH-responsive release (pH 5.5–6.5)	DOX	NCI-H1299 Non-Small Cell Lung Cancer	Active chemotaxis; 63.33% tumor cell apoptosis	[88]
Macrophage	Oral mRNA Delivery	Yeast-derived β-glucans targeting Dectin-1 receptor	Oral administration (Lymphatic transport)	mRNA (encoding cytokines)	Orthotopic 4T1 Triple-Negative Breast Cancer (TNBC) in BALB/c mice	Reprogrammed M2 to M1 phenotype; ~60% tumor volume reduction	[89]
Macrophage	Hitchhiking Nanomotors	Dectin-1 receptor on microfold cells	Oral administration	Zinc-DOX NPs	Orthotopic AK4.4 Pancreatic Ductal Adenocarcinoma in FVB mice	Induced MMP9/13 expression to degrade dense stromal fibrosis; suppressed metastasis	[90]
Neutrophil	Photo-inflammation Recruitment	Anti-CD11b antibody	NIR Laser (Photo-induced inflammation)	Paclitaxel Nanocrystals	Subcutaneous 3LL Lung Carcinoma & GL261 Glioma in C57BL/6 mice	Active transmigration across blood-tumor barrier; prolonged survival (~5% ID/g efficiency)	[91]
Neutrophil	Membrane Coating (Neutrosome)	LPS-activated membrane receptors	Biomimetic (Neutralizes TNF-α)	Cisplatin	Subcutaneous A549 Non-Small Cell Lung Cancer (NSCLC) in Balb/c nude mice	High tumor accumulation (>6-fold); neutralized TNF-α to restrict neutrophil infiltration; prolonged survival (64 days)	[92]
Neutrophil	CAR-Neutrophil	Chlorotoxin-targeted CAR	Hypoxia within tumor core	TPZ (Hypoxia-activated prodrug)	Orthotopic U87MG glioblastoma (GBM) in NOD-SCID mice	Crossed BBB; targeted delivery to GBM; significantly suppressed tumor growth and prolonged survival	[93]
Dendritic Cell	Immune Trafficking Bridge	Chemokines	Magnetic guidance	Magnetic Nanoprobes	Orthotopic GL261 Glioma in mice	Established "immune trafficking bridge" for B/T cell infiltration; inhibited tumor growth and prolonged survival	[94]
Dendritic Cell	Membrane Coating	Tumor-specific antigens	Biomimetic (BBB crossing)	Rapamycin	Orthotopic C6 Glioma in ICR mice	Efficient BBB crossing; activated T-cell immune response; significantly prolonged survival	[95]

macrophages are primarily characterized by their ability to mediate anti-inflammatory and immunosuppressive responses.1 This alternative activation is induced by a specific microenvironmental milieu containing M-CSF, IL-4, IL-10, IL-13, transforming growth factor-β (TGF-β), and glucocorticoids.[97] Following polarization, cells can secrete anti-inflammatory cytokines such as IL-10, IL-13, IL-4, Arginase-1 (Arg-1), and CD206, which play a role in host defense, wound healing, and tissue remodeling.[97] M2 macrophages can also facilitate tumor progression through several biological pathways, including the release of immunosuppressive factors like IL-10 and TGF-β, which impair the activity of other immune cells. Furthermore, these macrophages secrete vascular endothelial growth factor (VEGF), which enhances tumor angiogenesis.[100]

To address the transport barriers and negative feedback loops inherent in macrophage-based immunotherapy, Xu et al developed a spatial- and time-programmed polysaccharide nano-immunomodulator (Dex-RN). They used Dextran (Dex) as the hydrophilic nanocarrier backbone due to its intrinsic affinity for TAMs, utilizing the overexpression of mannose, Glucose Transporter 1 (GLUT1), and folic acid receptors on the macrophage surface for active targeting. Moreover, they utilized a dual-prodrug strategy with sequential drug release to repolarize immunosuppressive M2 macrophages into the anti-tumor M1 phenotype, ultimately achieving a 66% reduction in tumor growth and significantly minimizing systemic toxicity, particularly liver inflammation, by restricting immune activation specifically to the TME.[101] To further expand this repolarization strategy via gene therapy, Hu et al engineered a redox-responsive NP system (pIL-12+PLX@cR-PssPD) to simultaneously reprogram macrophages and activate cytotoxic immunity. To modulate the myeloid landscape, they delivered

PLX3397, which inhibited CSF-1 Receptor phosphorylation, thereby blocking the survival and differentiation of immunosuppressive M2 macrophages. Concurrently, they delivered a plasmid encoding IL-12 (pIL-12) to boost the antitumor activity of T cells and NK cells while fostering dendritic cell maturation. The system improved delivery precision through cyclic Arg-Gly-Asp-Phe-Lys (cRGD) surface modifications that targeted integrin and utilized disulfide bonds to trigger rapid payload release, specifically within the high-glutathione environment of the tumor cytoplasm.[102] While the previous strategies focused on reprogramming TAMs, an alternative approach utilizes macrophages as active delivery vehicles. Exploiting their natural homing ability, Hu et al developed a specialized "backpacking" system named DMPM containing Monocyte Chemoattractant Protein-1 (MCP-1) (DOX-loaded MPF127-MCP-1) The core of this system is the Pluronic F127 (PF127) copolymer, which was carboxylated and functionalized with the MCP-1 peptide. This specific peptide was selected as a high-affinity ligand for the C-C chemokine receptor type 2 (CCR2), utilizing the CCR2/MCP-1 signaling axis that naturally regulates macrophage recruitment to tumor sites. The authors employed a "backpacking" strategy wherein the NPs spontaneously bound to the surface of RAW264.7 macrophages via the MCP-1/CCR2 interaction, rather than being immediately internalized. By carrying the drug cargo on their surface, the macrophages retained their viability and chemotactic capabilities, effectively serving as "Trojan Horses" to actively transport the DOX. Once localized within the TME, the NPs exhibited pH-responsive behavior, releasing DOX rapidly in acidic conditions (pH 5.5–6.5) to induce significant tumor cell apoptosis (63.33%) while minimizing systemic toxicity.[88] Extending the Trojan horse concept to non-invasive administration routes, Luo et al demonstrated a "Trojan horse" strategy by engineering an oral mRNA delivery system for triple-negative breast cancer. By functionalizing lipid NPs with yeast-derived β-glucans, the authors specifically targeted the Dendritic cell-associated C-type lectin-1 (Dectin-1) receptor, which is highly expressed on intestinal macrophages. Following Dectin-1-mediated phagocytosis, these macrophages effectively loaded the mRNA cargo and migrated via the lymphatic system to the systemic circulation. Once localized within the TME, the carrier macrophages translated and secreted IFN-γ, which acted as an autocrine and paracrine signal to reprogram tumor-associated macrophages from an M2 to an M1 phenotype, resulting in significant tumor growth inhibition (~60% volume reduction).[89] Furthermore, in a parallel approach utilizing the same receptor-mediated uptake for chemotherapeutics, a study (2023) developed an oral macrophage-hitchhiking delivery system using β-glucan-functionalized zinc-DOX NPs (β-Glus-ZnD NPs). This strategy utilized the abundance of Dectin-1 receptors on intestinal microfold cells and macrophages to facilitate transcytosis across the intestinal epithelium and subsequent phagocytosis by endogenous macrophages within the lymphatic system. The internalization of Glus-ZnD NPs reprograms tumor-associated macrophages from a pro-tumor M2-like phenotype to an anti-tumor M1-like phenotype and induces the expression of MMP9 and MMP13, which degrade the dense stromal fibrosis that typically hinders drug penetration.[90]

Moving beyond synthetic and mammalian cell-based carriers, Jiang et al developed a hypoxia-responsive "living material" using engineered *Escherichia coli Nissle* 1917 to overcome transport barriers in solid tumors. By equipping the bacteria with a hypoxic lytic circuit, the system ensures bacterial lysis specifically within the necrotic tumor core. This lysis releases intracellular adjuvants, including DNA and flagellin, which activate Toll-like receptor 4 (TLR4) on infiltrating macrophages. This activation successfully triggers the repolarization of TAMs from the immunosuppressive M2 phenotype to the anti-tumor M1 phenotype, thereby enhancing the efficacy of the DOX.[103]

Neutrophil

Neutrophils originate from hematopoietic stem cells (HSCs) in the bone marrow. This developmental pathway begins with HSCs differentiating into common myeloid progenitors (CMPs), which then progress into granulocyte–monocyte progenitors (GMPs), ultimately maturing into mature neutrophils.[104] They exhibit marked heterogeneity and functional duality in response to cancer. Driven by specific signaling cues originating from the TME, they differentiate into opposing phenotypes within the classification of tumor-associated neutrophils (TANs): N1 TANs, which exert anti-neoplastic effects, and N2 TANs, which facilitate tumor progression.[105] N1 TANs mediate anti-tumor effects by releasing cytotoxic factors, stimulating anti-tumor immune responses, and contributing to antibody-dependent cytotoxicity. N2 TANs facilitate tumor initiation, growth, and progression through multiple mechanisms, including inducing genotoxic stress and malignant transformation, promoting tumor cell proliferation and angiogenesis, releasing neutrophil extracellular traps (NETs), accelerating epithelial–mesenchymal transition, remodeling the ECM, and preparing pre-metastatic niches, as well as driving immunosuppression.[106] These N2-associated mechanisms present significant transport barriers.

Specifically, NETs (comprising sticky DNA decorated with proteases) act as a dense physical barrier that entraps NPs via electrostatic and steric interactions, thereby preventing deep tissue penetration.[107] Furthermore, ECM remodeling driven by N2 neutrophils increases IFP, severely limiting the passive diffusion of nanotherapeutics.[106] However, recent "Trojan horse" strategies exploit neutrophils' inherent chemotactic ability to traverse biological barriers. By loading NPs into neutrophils (or hitchhiking on their surface), therapeutic payloads can be actively transported across the vessel wall and into the tumor core, bypassing the barriers that typically hinder free NPs.[108] One primary application of neutrophils in nanomedicine-based tumor therapy is their use as drug delivery systems, along with their derivatives. Since circulating neutrophils can cross biological barriers, they have been suggested as a hitchhiking approach for targeted drug delivery. For example, Ding et al engineered sialic-acid–stearic-acid conjugates to modify the surface of epirubicin-loaded liposomes (EPI-SL), thereby increasing their uptake by circulating neutrophils and monocytes. Upon exposure to tumor-derived inflammatory cytokines, these EPI-SL–loaded N/Ms preferentially home to tumor sites and promote the localized accumulation of the drug. This strategy significantly suppressed, and in some cases eliminated, tumor growth in murine models, indicating that neutrophil/monocyte-assisted transport can markedly enhance the tumor specificity and therapeutic performance of epirubicin.[109] To actively improve the recruitment of these carrier cells to the tumor site, Su et al used photoinduced inflammation to recruit neutrophils as active transporters for anti-CD11b antibody-coated paclitaxel (PTX) nanocrystals (Ab/PTX NC). In this system, laser irradiation triggers an acute inflammatory response that upregulates CD11b on circulating neutrophils, allowing them to specifically internalize the nanocrystals and actively transmigrate across the blood-tumor barrier.[91] Rather than using live neutrophils, an alternative biomimetic strategy involves coating nanoparticles with neutrophil membranes to mimic their natural behavior. Adopting this approach, Wu et al proposed a pluripotential neutrophil-mimic nanovehicle, Neutrosome(L), composed of cisplatin-loaded liposomes incorporated with the membranes of neutrophils that were activated explicitly via LPS stimulation By utilizing the upregulated adhesion proteins and receptors on activated membranes, this system mimics the natural inflammatory tropism of neutrophils, enabling deep tumor penetration and significantly higher drug accumulation. Furthermore, Neutrosome(L) acts as a trap to neutralize inflammatory cytokines such as TNF-α, thereby restricting TAN infiltration and remodeling the microenvironment, ultimately potentiating the antitumor effects of chemotherapy while reducing systemic toxicity.[92] Integrating nanotechnology with genetic engineering for precise targeting, Chang et al developed a renewable platform using human pluripotent stem cells (hPSCs) engineered with a Chlorotoxin-targeted Chimeric Antigen Receptor (CLTX-CAR). These engineered CAR-neutrophils were utilized as biomimetic carriers for rough mesoporous silica NPs (R-SiO_2) loaded with the hypoxia-activated prodrug tirapazamine (TPZ). Utilizing rough-surfaced NPs, which neutrophils preferentially phagocytosed over smooth counterparts due to their resemblance to microbial pathogens, enabling high drug-loading capacity without compromising chemotaxis.[93]

Dendritic Cells

Dendritic cells (DCs) are essential APCs that manage the anti-tumor T cell reaction through various mechanisms, including the recruitment of $CXCR3^+$ cytotoxic T lymphocytes (CTLs) into the TME, which is mediated by chemokines CXCL9 and CXCL10, which are produced by conventional type 1 dendritic cells (cDC1s). This signaling pathway is critically important; NPs designed to deliver immunomodulatory agents, such as Stimulator of Interferon Genes (STING) agonists, can specifically target cDC1s to amplify CXCL9 and CXCL10 production, thereby overcoming the exclusion of T cells from the tumor core. Additionally, migration of tumor-infiltrating dendritic cells (TIDCs) to lymph nodes for the presentation of antigens to CD8+ T naïve cells.[110] This migratory pathway is increasingly utilized by "cellular hitchhiking" strategies, in which NPs internalized by DCs are actively transported from the tumor stroma to the lymph nodes, effectively using the cell as a vehicle to bypass physiological barriers that restrict passive diffusion. Furthermore, DCs participate in "cross-dressing," or trogocytosis, with tumor cells. This mechanism involves a transfer of tumor-derived extracellular vesicles (EVs) and intercellular plasma membrane fragments containing intact antigenic major histocompatibility complex (MHC) peptide-MHC complexes to DCs. This facilitates the immediate activation of $CD8^+$ T lymphocytes without the need for additional antigen processing.[111] Recent studies have mimicked this mechanism by developing DC-membrane-coated NPs that act as pseudo-APCs to directly present antigens and sustain immune activation even when endogenous DC function is compromised. For instance, Zhang et al developed a biomimetic

nanotheranostic system by engineering bone marrow-derived DCs as "Trojan horse" vehicles to overcome the restricted immune infiltration in glioma. In this methodology, DCs were labeled with magnetic-fluorescent nanoprobes (internally loaded with the chemokines CXCL13 and CCL21. Once integrated, the DCs released the encapsulated chemokines to establish an "immune trafficking bridge," which facilitated the centripetal redistribution of effector $B220^+$ B cells and $CD8^+$ T cells into the tumor core, while simultaneously permitting non-invasive spatiotemporal monitoring of mature tertiary lymphoid structures (mTLS) formation via dual-mode magnetic resonance imaging (MRI).[94]

While the previously mentioned strategy improved immune trafficking, effective treatment of glioma also requires bypassing the physical barrier of the brain. Addressing the dual challenge posed by the BBB and the immunosuppressive microenvironment, Ma et al developed a biomimetic nanoplatform comprising a rapamycin (RAPA)-loaded poly(lactic-co-glycolic acid) (PLGA) core coated with activated mature DC membranes (aDCM@PLGA/RAPA). The activated DCs were generated by co-culturing mouse bone marrow-derived DCs with C6 glioma cell lysate, thereby inducing the presentation of tumor-specific antigens (pMHC molecules) and the upregulation of costimulatory markers (CD80/CD86) on the DC surface before membrane extraction. This nanosystem remodeled the immune microenvironment by directly activating naive T cells and indirectly promoting host DC maturation, leading to increased infiltration of CD8+ T cells and NK cells, thereby significantly prolonging survival in orthotopic glioma-bearing mice.[95]

Moving from glioma to colorectal cancer, where the immunosuppressive TME severely inhibits DC maturation, a biomimetic nano-vaccine was developed utilizing gambogic acid (GA)-loaded PLGA NPs coated with cancer cell membranes. By co-delivering tumor antigens retained on the membrane and the immune-adjuvant GA, this system effectively targets and activates DCs, achieving a 4-fold increase in maturation rates in vitro, allowing the NPs to accumulate specifically at the tumor site while evading liver clearance, ultimately remodeling the immune microenvironment to enhance CD8+ T cell infiltration and synergistic tumor inhibition with anti-PD-1 therapy.[112]

To further potentiate therapeutic outcomes by synergizing nanotechnology with adoptive cell therapy, a "CATCH" strategy was developed that integrates lipid NPS (LNP)-mRNA technology with DC therapy. This method involves intratumoral injection of LNPs encoding CD40 ligand (CD40L) to induce immunogenic cell death and CD40L expression in tumor cells, followed by the adoptive transfer of DCs engineered ex vivo via separate optimized LNPs (DIM7S) to overexpress CD40. This approach improves efficacy by establishing a synergistic activation loop where tumor-expressed CD40L stimulates the injected CD40-DCs, leading to enhanced antigen presentation, potent $CD8^+$ T cell infiltration, and the complete eradication of established tumors with long-term immunological memory.[113]

Physiological Barriers: The Blood-Brain Barrier (BBB)

Blood and brain tissue are separated by a particular physiological barrier called the BBB. It mainly consists of endothelial cells, basement membranes, pericytes, astrocytes, and various junctional structures, such as tight junctions (TJs) and adhesion junctions (AJs).[114] Brain microvascular endothelial cells (BMECs) are a key cellular element of the BBB. These endothelial cells are linked to one another through tight junctions, which are assembled from transmembrane proteins including occludin, claudin-3, and claudin-5 and cytoplasmic scaffolding proteins, including zonula occludens-1, −2, and −3 (ZO-1, ZO-2, ZO-3).[115] Critically enhance the selective permeability of the BBB by limiting the paracellular diffusion of most hydrophilic substances and high-molecular-weight compounds.[116] BMECs express a variety of membrane receptors and transporters that facilitate the active entry of essential nutrients and metabolites across the BBB.[117] Additionally, they have specific characteristics, including low levels of non-specific cytosis (cytosolic drinking), poor windowing, and limited paracellular diffusion. Another essential part of the BBB is the basement membrane, which is secreted by both astrocytes and BMECs. Laminin-1, 2, 4, and 5, collagen IV, and glycoproteins make up the majority of it.[118]

In addition to protecting the brain from infections and poisons, the BBB restricts drug penetration to lipophilic, low-molecular-weight molecules (less than 400–500 Da).[119] This indicates that almost all major therapeutic molecules, including viral vectors, anti-sense oligonucleotides, and monoclonal antibodies, as well as about 98% of tiny compounds, are unable to cross this barrier.[119] For instance, the maximum tumor-to-blood concentration ratio attained is less than 20%, even though the standard-of-care temozolomide (TMZ), a 194 Da lipophilic molecule, falls within the permeability parameters.[120] The transition from a healthy Blood-Brain Barrier to a Blood-Brain Tumor Barrier (BBTB) in glioblastoma (GBM) is characterized by significant structural heterogeneity, where the tumor core creates a leaky, immature

 https://doi.org/10.2147/IJN.S563233

vasculature. At the same time, the peripheral areas maintain a functional barrier.[121] This inconsistency, combined with the upregulation of efflux transporters, severely restricts the distribution of therapeutics to the invasive tumor edges.[122] Therefore, developing delivery systems capable of traversing the intact barrier is essential for treating the diffuse borders of the malignancy.

Among emerging strategies to overcome this barrier, exosome-mediated delivery has gained prominence for its inherent biocompatibility and transport capabilities. Utilizing this natural carrier, Wang et al developed a redox-responsive, engineered exosome delivery system loaded with DOX (Pep2-Exos-DOX). The authors selected exosomes derived from BV2 mouse microglial cells as the carrier. They demonstrated that these vesicles could effectively breach the BBB primarily through cholesterol-dependent, clathrin-independent endocytosis and macropinocytosis. To improve delivery efficiency and prevent drug loss during circulation, the exosome surface was modified with a functional amphiphilic oligopeptide (Pep2) containing cysteine residues. These peptides formed disulfide cross-links upon mild oxidation, effectively "locking" the drug within the vesicle until it reached the TME, where high GSH levels reduced the bonds, triggering release.[123]

While the previous study focused on hydrophilic drugs such as DOX, delivering hydrophobic agents, such as rapamycin, presents additional solubility challenges. To address these physicochemical limitations within the context of BBB delivery, Song et al engineered a biomimetic delivery system by encapsulating rapamycin into MSC-derived exosomes (Exo-Rapa) using a real-time incubation method optimized via response surface methodology (RSM) To overcome the BBB, they employed the inherent permeability and endocytic capabilities of MSC-derived exosomes, demonstrating that Exo-Rapa successfully crossed an in vitro BBB monolayer and accumulated in the brain tissue of orthotopic GBM mice. In contrast, free rapamycin remained undetectable in the brain. This system further enhanced delivery efficacy through a pH-responsive release mechanism, which triggered rapid drug release in the acidic TME (pH=5.5) while maintaining stability under physiological conditions, ultimately inhibiting angiogenesis via the VEGF/VEGFR axis and prolonging survival in GBM-bearing mice.[124]

Beyond endogenous carriers like exosomes, synthetic surface engineering offers precise control over transport mechanisms, particularly for chemotherapeutics with high systemic toxicity. Illustrating this approach for PTX, a recent study engineered a dual-responsive nanoplatform by coating a GSH-sensitive chitosan-PTX core with a pH-labile poly(2-methacryloyloxyethyl phosphorylcholine) (PMPC) shell via a Schiff base reaction. To overcome the BBB, the system utilized the choline-analogous properties of the PMPC shell, which facilitated transcytosis across brain endothelial cells through specific binding to nicotinic acetylcholine receptors and choline transporters, effectively bypassing the barrier via receptor-mediated transport. This design further improved delivery efficacy through a sequential response mechanism, where the acidic TME (pH<6.8) triggered shell detachment to expose a positively charged core for deep tissue penetration, followed by GSH-mediated disulfide cleavage for intracellular drug release, resulting in significantly suppressed tumor growth and extended survival in orthotopic GBM models.[125]

Moving from small-molecule chemotherapy to immunotherapy, delivering large biologic drugs requires overcoming even stricter size and transport constraints. Addressing this challenge, a recent study engineered a biomimetic nanoplatform (aLy-6C-LAMP) by coating a Ly-6C-targeted cationic liposome core containing a PD-L1 trap plasmid with a red blood cell membrane (RBCM). To overcome the BBB, the system utilized a "Trojan horse" strategy mediated by monocytic MDSCs, which facilitated transport across the barrier by exploiting the inflammatory recruitment of these cells via upregulated adhesion molecules (VCAM-1 and ICAM-1) on brain endothelium post-chemoradiotherapy. This design further improved delivery efficacy through the CD47-mediated long circulation of the RBCM shell, which ensured efficient loading of splenic M-MDSCs and subsequent intratumoral secretion of the PD-L1 trap protein, thereby reactivating antitumor immunity and significantly extending median survival in recurrent GBM models.[126] TMZ resistance poses a significant challenge in GBM treatment, yet the delivery of reversing agents is frequently hindered by the blood-brain barrier (BBB). A recent study engineered a "fixed-point cleaved" biomimetic nanosystem (S@TTNMs) by coating the Phosphoinositide 3-kinase (PI3K) inhibitor SF2523 with a neutrophil membrane modified with Tryptophan and a fusion peptide. To overcome the BBB, the system employed a dual-targeting strategy combining carrier-mediated transcytosis via the L-type amino acid transporter-1 (LAT1) and receptor-mediated transcytosis via the TGN peptide. Finally, therapeutic success in GBM is often limited not just by delivery, but by the development of drug resistance (eg, to TMZ) To tackle both penetration and resistance simultaneously, Gu et al improved the efficacy through spatiotemporally sequential surface transformations: the high expression of γ-GT in the glioma microenvironment triggered the cleavage of the fusion peptide to expose the tumor-targeting A7R ligand, while the acidic tumor pH subsequently detached these modifications to utilize the neutrophil membrane's inflammatory chemotaxis for

deep penetration, ultimately inhibiting the PI3K/ mammalian target of rapamycin (mTOR)/ nuclear factor kappa-light-chain-enhancer of activated B cells (NF-κB) pathway to sensitize resistant cells[127] To address these physiological challenges, various nanoparticle-based strategies have been developed A comprehensive overview of these barriers and the corresponding targeted strategy is presented in Table 2.

Programmed Nanoparticle Delivery Strategies for Enhanced Tumor Penetration

Programmed NP delivery systems are designed to overcome the physiological barriers of solid tumors by responding dynamically to internal tumor microenvironmental cues or external stimuli These innovative systems aim to enhance intratumoral penetration and therapeutic efficacy by enabling controlled release, deeper tissue access, and improved cellular uptake Key strategies include stimulus-responsive size transformation, surface modification to enhance transport and evasion of biological barriers, and ligand-mediated targeting for selective cellular uptake (86).

Size-Switchable Nanoparticles

The therapeutic efficacy of nanocarriers is governed by a fundamental trade-off between systemic circulation and intratumoral transport, dictated primarily by particle size.[131,132] Large nanoparticles (>50 nm) are advantageous for prolonging circulation and exploiting the EPR effect for tumor accumulation.[133,134] However, comparative analyses indicate that this larger hydrodynamic diameter significantly restricts diffusion through the dense ECM and elevated IFP of the tumor core.[41] In contrast, ultrasmall nanoparticles (<20 nm) demonstrate superior diffusivity and deep tissue penetration but are limited by rapid renal clearance and poor tumor retention.[132,135] Therefore, size-switchable systems are designed to strategically toggle between these two distinct biological behaviors, maintaining a "retention-favored" large size in circulation and transforming into a "penetration-favored" small size specifically within the TME.

To implement this strategy, TME-responsive NPs are engineered to undergo volume reduction in response to specific microenvironmental cues or external stimuli. This transformation effectively resolves the steric hindrance posed by the ECM, enabling the generated smaller components to access deep tumor regions that remain impermeable to the larger parent nanocarriers.[136] Figure 3 illustrates this adaptive transport mechanism, highlighting how dynamic size adaptation integrates the pharmacokinetic stability of larger particles with the superior diffusivity of smaller ones.

Table 2 Overview of Physiological Barriers in Solid Tumors and Nanoparticle Strategies

Barrier	Biophysical Characteristic	Challenge for Nanoparticles (NPs)	Strategy	Ref.
Dense ECM	High density of collagen fibers and hyaluronic acid	Steric hindrance limits the diffusion and deep penetration of NPs	Enzymatic Degradation (eg, Collagenase, Hyaluronidase) or Size-Switching (Shrinking)	[46,128]
Elevated IFP	High hydrostatic pressure caused by leaky vessels and a lack of lymphatic drainage	Opposes convective transport; pushes drugs out of the tumor	Vascular Normalization (eg, VEGFR inhibitors like Cediranib) to restore pressure gradients	[21,81]
Abnormal Vasculature	Disorganized and leaky blood vessels	Heterogeneous blood flow; limited perfusion to the tumor core	Shape-Transformable NPs (eg, Spheres to Nanofibers) or Size-Switching	[74,129]
Blood-brain barrier	Tight junctions between endothelial cells and astrocyte end-feet	Blocks paracellular transport of >98% of therapeutic molecules	Receptor-Mediated Transcytosis (eg, via Choline transporters) or Exosome Delivery	[123,125]
Hypoxia	Low oxygen levels (<10 mmHg) in the tumor core	Induces drug resistance and alters metabolic pathways	Hypoxia-Responsive Linkers (eg, Azobenzene cleavage) trigger disassembly	[93,130]
Immune Clearance	Presence of phagocytic cells (Macrophages, Neutrophils)	Rapid clearance of NPs before reaching the target	"Trojan Horse" Cellular Hitchhiking or Biomimetic Membrane Coating	[88,92]

https://doi.org/10.2147/IJN.S563233

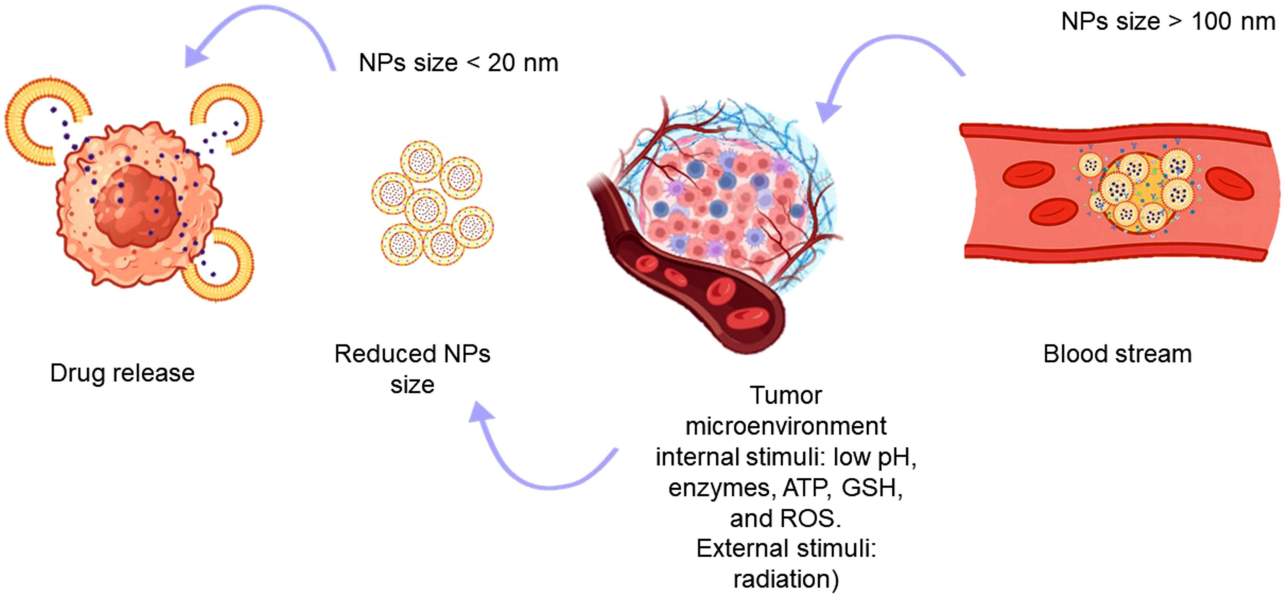

Figure 3 Schematic representation of the size-transformable nanocarrier mechanism. Nanoparticles (NPs) circulate in the bloodstream at larger sizes (>100 nm) to enhance stability and prolong circulation. Upon exposure to tumor microenvironment stimuli (eg, low pH, enzymes, ATP, GSH, ROS, and external radiation), NPs shrink to smaller sizes (<20 nm) to improve tumor penetration.

pH-Sensitive Size-Switchable Nanoparticles

The acidic extracellular pH of solid tumors (typically pH ~6.5–7.2) is one of the most exploited features of the TME for targeted drug delivery.[137,138] This pH difference between tumor and normal tissues has been widely used to design size-switchable NPs that can respond to acidity by disassembling, shrinking, or activating payload release.[139] Such systems offer the advantage of prolonged systemic circulation in their original form and enhanced deep tissue penetration upon transformation, ultimately improving therapeutic efficacy.[75]

In a notable study, Li et al reported a smart, stimuli-responsive nanocluster synthesized via molecular self-assembly with an initial size of 100 nm, designed to deliver cisplatin into tumor cells. These clustered NPs consist of a platinum (Pt) prodrug-conjugated PAMAM-graft-polycaprolactone (PCL-CDM-PAMAM/Pt), combined with a PCL homopolymer and a poly(ethylene glycol)-b-poly(ε-caprolactone) (PEG-b-PCL) copolymer. Upon accumulation in tumor regions, the mildly acidic extracellular tumor environment (pH ~6.5–7.2) triggers the release of Pt-prodrug-conjugated PAMAM dendrimers with a reduced size of approximately 5 nm. While the initial 100 nm size facilitated tumor accumulation via the EPR effect, it was the transition to the 5 nm size that enabled the drug to breach the dense stromal barrier, achieving a penetration depth that was impossible for the larger clusters.[67] While single-stimulus systems are effective, the complexity of the intracellular environment often necessitates multi-stage responsiveness to achieve precise drug release. To address this, Hou et al introduced multi-pocket NPs (MPNs) that respond to both pH and redox stimuli These NPs, fabricated through self-assembly and crosslinking of amphiphilic mPEG-LA conjugates, have an initial size of ~170 nm. At the tumor site, enhanced PEG solubility under acidic conditions destabilizes the supramolecular structure, disassembling the MPNs into smaller units (<20 nm) that can penetrate more deeply into tumor tissues. This size reduction was critical for therapeutic success; the initial 170 nm size ensured extended circulation, whereas the transformed <20 nm particles could navigate the narrow interstitial spaces to reach the tumor core (Figure 4).[75]

Beyond therapeutic delivery, real-time monitoring of nanoparticle disintegration and drug release is crucial for optimizing treatment regimens. Integrating diagnostics with therapy, Hao et al developed dual-responsive polyprodrug NPs (SPNs) designed to respond to both the acidic TME and the reductive intracellular milieu. These SPNs were synthesized via co-assembly of a negatively charged block copolymer, PDMA-b-P(AEMA-DA), and a positively charged three-armed star-shaped polyprodrug, t-P(CPTM-co-DTPA(Gd)-co-CS)-b-PGEMA. The NPs exhibited high CPT loading (~28.6 wt%) through disulfide linkages within their hydrophobic cores. A key feature of these SPNs was their acid-triggered size

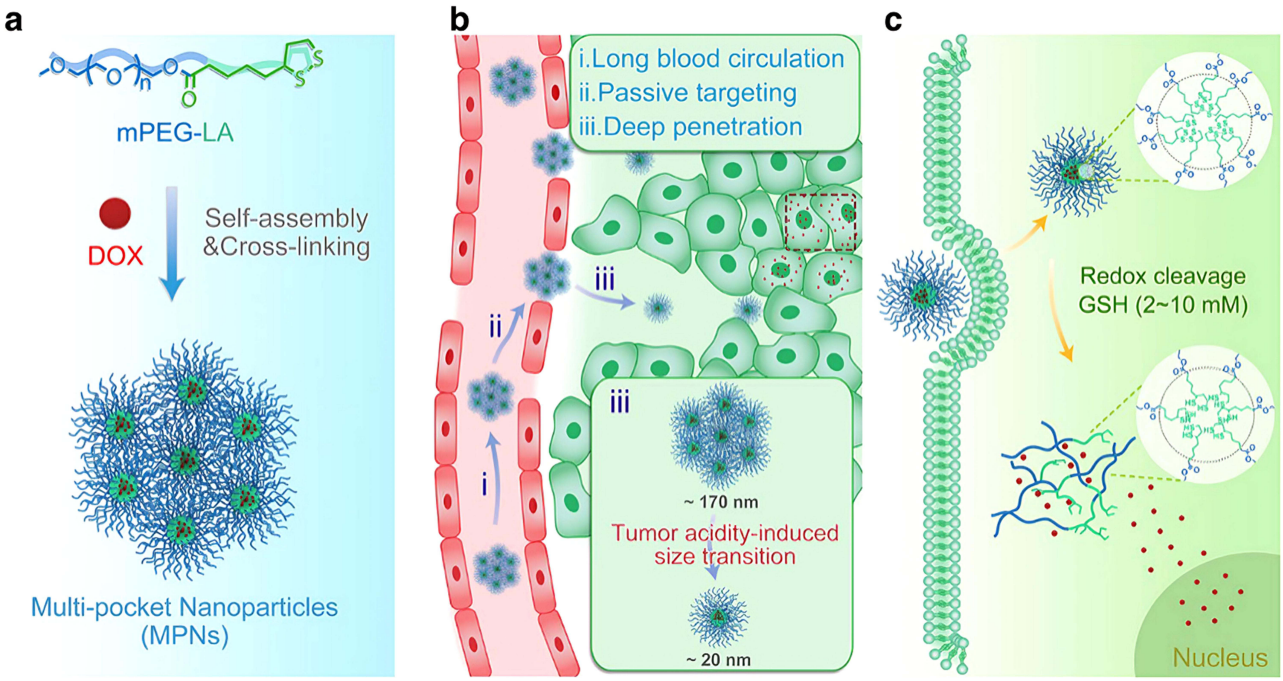

Figure 4 Schematic illustration of the design, delivery mechanism, and intracellular drug release behavior of MPNs for doxorubicin (DOX) delivery. (**a**) MPNs are synthesized via self-assembly and cross-linking of amphiphilic mPEG-LA conjugates, encapsulating DOX within their supramolecular network. (**b**) In vivo behavior of DOX-loaded MPNs: (i) The PEGylated, large-sized (~170 nm) MPNs exhibit prolonged blood circulation by evading immune clearance. (ii) Extended circulation enables passive targeting and accumulation at tumor sites through the EPR effect. (iii) In the mildly acidic TME, MPNs undergo a pH-induced size transition, disassembling into smaller NPs (~20 nm) that facilitate deeper tumor penetration. (**c**) Inside tumor cells, high intracellular GSH (2–10 mM) levels trigger redox-responsive cleavage of disulfide bonds, leading to the disintegration of the NP structure and subsequent release of DOX into the cytoplasm and nucleus. Adapted with permission from.[75]

transformation; under mildly acidic tumor conditions (pH ~6.8), the acid-labile outer shell (PDMA-b-P(AEMA-DA)) detached, releasing smaller, positively charged polyprodrug NPs (~10–20 nm). This size reduction significantly enhanced tumor penetration and cellular internalization. Subsequently, the reductive cytosolic environment triggered the release of parent CPT from the core. Importantly, Diethylenetriaminepentaacetic acid (DTPA) (Gd) units embedded within the polyprodrug matrix served as MRI contrast agents, enabling real-time monitoring of the SPNs' disintegration, biodistribution, and drug release via cascade-enhanced MR signals.[140] To address the specific challenge of multidrug resistance (MDR), which often limits the efficacy of chemotherapy in deep tumor regions, Feng et al developed dual pH/redox-responsive multiscale NPs (DMA-NPs) to overcome MDR. These particles consisted of a poly (ethylene glycol)- poly (amidoamine) dendrimer (PEG-PAH-DMA) polymeric shell and a core of dendrimeric PPT prodrug (PAMAM-ss-PPT). The system maintained a ~170 nm size and a negative charge under normal conditions. In the acidic tumor environment, electrostatic repulsion facilitated the release of positively charged PAMAM-ss-PPT, resulting in a reduced particle size and improved tumor penetration. This transformation allowed the particles to penetrate deeply into multidrug-resistant tumor regions, overcoming the diffusion limits that typically trap larger nanocarriers at the tumor periphery.[141] While biochemical stimuli rely mainly on passive diffusion, integrating external physical forces can further boost penetration into dense tissues. Using magnetic actuation to drive transport, Zhu et al developed a multifunctional nanocarrier system for deep tumor delivery of DOX, incorporating ferrimagnetic nanocubes, a deformable polyphosphoester core, and a pH-sensitive transactivator of transcription (DAT-PPED&F) responsive to the tumor extracellular environment. The nanocarriers, with an initial size of ~180 nm, were actuated magnetically to facilitate vascular escape and enhance accumulation at the tumor site. Upon arrival, the soft, flowable polyphosphoester core enabled the NPs to deform and traverse narrow interstitial spaces (~100 nm) within the dense tumor matrix, achieving greater penetration compared to conventional rigid carriers. Moreover, the DAT-PPED&F component, activated by acidic pH, reinitiated and enhanced the cellular uptake of doxorubicin. The integration of ferrimagnetic nanocubes also enabled external magnetic-field guidance and propulsion, offering spatial control over NP delivery and improving intratumoral distribution.[142]

https://doi.org/10.2147/IJN.S563233

Applying the pH-triggered size-switching concept to photodynamic therapy (PDT) to enhance singlet oxygen generation deep within tumors, Xu et al developed PEG-Ce6@PAEMA nanoassemblies for membrane-targeted PDT. These structures (~103.6 nm) comprise PEG- Ce6 and a pH-sensitive PAEMA polymer. Under tumor acidity, rapid protonation of PAEMA led to disassembly, releasing small PEG-Ce6 molecules (~12.9 nm). This transition allowed the photosensitizer to bypass the stromal barrier and attach directly to cancer cell membranes, maximizing phototoxicity deep within the tumor.[143] Collectively, these pH-sensitive, size-switchable NPs represent a powerful class of innovative drug delivery systems that address key challenges in tumor treatment. By maintaining circulation stability and transforming in response to tumor acidity, these systems enable improved tumor targeting, enhanced penetration, and controlled drug release.

Hyaluronidase-Sensitive Size-Switchable Nanoparticles

Hyaluronidase is an overexpressed enzyme in many tumor types, particularly in highly metastatic cancers, where its concentration is markedly elevated.[144] This feature has been effectively exploited in the design of enzyme-sensitive, size-switchable NPs for tumor-targeted drug delivery.[145] Liu et al developed a multifunctional delivery system to transport indocyanine green (ICG), an NIR imaging agent, to tumor tissues. They first synthesized cationic, red-emitting BSA-protected gold nanoclusters (AuNC@CBSA) to co-load ICG, forming AuNC@CBSA-ICG. This was subsequently coated with negatively charged HA, resulting in the formation of larger NPs (AuNC@CBSA-ICG@HA) to enhance circulation time and stability. The HA coating not only enabled prolonged systemic circulation but also conferred active tumor-targeting capability through HA's affinity for CD44 receptors, which are often overexpressed on cancer cells, a modification known to enhance endocytosis and improve selectivity towards cancer cells.[146] Upon reaching the TME, hyaluronidase-mediated degradation of HA reduced NP size. This transition was pivotal: the bulky HA shell prevented renal clearance. It facilitated CD44-mediated accumulation, while the enzyme-stripped small cores could freely diffuse into the dense tumor matrix, achieving deep tissue distribution that the large precursor could not.[128] While HA provides targeting via CD44 receptors, improving specificity often requires dual-targeting strategies. Addressing this, Ma et al developed a HA-coated NP platform for the delivery of DOX, composed of dendrigraft poly-L-lysine (DGL) conjugated with glycyrrhetinic acid (GA), cyclohexane dicarboxylic anhydride (CDA), and DOX, and finally coated with HA (DGL-GA-CDA-DOX-HA). The initial NP size was 182.5 nm, which decreased significantly to 47.7 nm upon exposure to hyaluronidase. This significant size reduction was the primary driver for overcoming the stromal barrier, enabling the drug to penetrate the deep tumor parenchyma where the original large nanoparticles would have been trapped by the ECM.[147] Demonstrating the versatility of this enzyme-triggered approach for theranostic applications, Yu et al designed HA-based NPs using cationic BSA-protected gold nanoclusters loaded with ICG (AuNC@CBSA-ICG@HA). This system also demonstrated enzyme-triggered size reduction, from an initial diameter of 200 nm to 50 nm, in the presence of hyaluronidase. This dynamic alteration enabled the system to employ the EPR effect for accumulation while ensuring that the payload was not sequestered in the perivascular space but delivered deep into the tumor core.[21] Cumulatively, these studies underscore that while ligand-mediated targeting improves accumulation, it is the enzyme-triggered size reduction that ultimately governs the depth of intratumoral distribution, achieving efficient therapeutic outcomes through structural modulation.

Reactive Oxygen Species (ROS)-Sensitive Size-Switchable Nanoparticles

ROS-sensitive nanocarriers have emerged as promising tools for tumor-specific drug delivery due to the elevated oxidative stress levels within tumor tissues.[148,149] These systems can respond to endogenous ROS or externally induced ROS generation to trigger structural disassembly, drug release, and improved tissue penetration.[150] Shen et al developed a multifunctional ROS-responsive nano-delivery platform based on an amphiphilic block copolymer, PEG-b-poly (propylene sulfide) (PEG-PPS), which was used to form micelles encapsulating Fe_3O_4 NPs and hypocrellin (HC), a sonosensitizer.[151] Upon ultrasound (US) irradiation, HC generates ROS, which subsequently trigger the oxidation-sensitive disintegration of the micelles. This response leads to a significant reduction in size and the release of small Fe_3O_4 NPs. The released Fe_3O_4 then catalyzes a Fenton reaction, wherein hydrogen peroxide (H_2O_2) is converted into hydroxyl radicals (•OH), thereby initiating lipid peroxidation and inducing ferroptosis; an iron-dependent type of

programmed cell death identified by a formation of ROS and lipid peroxides. Furthermore, tumor cells are known to express elevated intracellular GSH levels, which can scavenge ROS and compromise the efficacy of ROS-based therapies, such as sonodynamic therapy (SDT). Notably, Fe^{3+} can react with GSH to generate Fe^{2+}, which, in turn, perpetuates the Fenton cycle, amplifying ROS production and reinforcing ferroptotic activity. The micelles exhibited an initial diameter of approximately 150 nm. Upon US-triggered disassembly, the released nanostructures were reduced in size to ~70 nm or smaller. This size transition was essential for efficacy; the initial 150 nm size facilitated passive accumulation, while the reduced 70 nm fragments significantly improved intratumoral dispersion, allowing the therapeutic agents to penetrate regions inaccessible to the intact micelles.[151] In another approach, instead of relying on external ultrasound, endogenous chemical amplification of ROS can also trigger disassembly. Exploring this chemo-centric approach, Li et al engineered a dual pH/ROS-responsive nanoplatform termed RLPA-NPs, which integrates tumor-penetrating capabilities with triggered drug release mechanisms, highlighting the capacity of smart micelles for synergistic co-delivery.[152,153] The system comprises a pH-sensitive polymer, octadecylamine-poly(aspartate-1-(3-amino-propyl) imidazole) [OA-P(Asp-API)], co-assembled with a ROS-generating agent β-lapachone (Lap), and a ROS-responsive PTX prodrug. This cascade of events effectively transformed the bulky nanocarrier into smaller therapeutic units, enabling deep penetration of tumor tissue that the original micellar structure could not achieve due to steric hindrance in the ECM.[152] Alternatively, for tumors treated with radiotherapy, X-rays can serve as the external trigger for ROS generation and nanoparticle activation. Utilizing this mechanism, Lin et al constructed GSH-responsive JNP Ve from gold-manganese oxide NPs that undergo self-assembly into ~100 nm vesicles. Upon exposure to X-ray irradiation, the vesicles disassembled into smaller gold NPs and Mn^{2+} ions. This structural collapse was the key determinant of therapeutic success: the 100 nm vesicles ensured stability during circulation, whereas the post-irradiation small fragments could deeply penetrate the tumor parenchyma, enhancing radiosensitization well beyond the perivascular zone.[74] Together, these studies underscore the potential of ROS-sensitive, size-switchable nanocarriers. By integrating ROS amplification with dynamic size reduction, these systems solve the transport bottleneck, proving that smaller post-trigger particles are far more effective at navigating the oxidative tumor microenvironment than their larger precursors.

NIR-Induced Size-Switchable Nanoparticles

NIR light-responsive nanocarriers have attracted considerable attention due to their non-invasive activation, deep tissue penetration, and the ability to enable spatiotemporal control over drug release.[154,155] NIR irradiation can trigger photothermal and photodynamic effects, which in turn induce size shrinkage, micelle disassembly, or structural transformation of nanocarriers, thereby improving tumor penetration and therapeutic outcomes.[156–159] Wu et al developed a NIR-responsive nanomicelle system with an initial particle size of approximately 101 nm for DOX delivery. The system consisted of gold nanorods encapsulated within a thermo-responsive copolymer shell, poly(acrylamide-co-acrylonitrile)-graft-polyethylene glycol-lipoic acid [p(AAm-co-AN)-g-PEG-LA], which exhibits upper-critical-solution-temperature behavior. Upon NIR laser irradiation, the gold nanorods converted light into heat, demonstrating the intrinsic photothermal capacity of gold nanostructures to enhance chemotherapeutic cytotoxicity[160] and induce photothermal ablation of surface tumor tissues. Simultaneously, the elevated local temperature triggered micellar disassembly, leading to the formation of ultrasmall micelles (~7 nm). This size reduction was the defining factor for efficacy. While the initial 101 nm micelles were confined to the perivascular space due to their size, the transformed 7 nm units utilized their reduced steric bulk to diffuse extensively throughout the dense tumor tissue.[79] Extending the photothermal strategy beyond physical penetration to immune modulation, Cong et al designed a bioinspired "nanoconverter" to transform the immunosuppressive TME into an immunostimulatory one. They developed a nanovesicle system termed PTX/PDA@M-C6, consisting of PTX encapsulated within a PDA core and coated with a C6-ceramide-modified tumor cell membrane. The system self-assembled into vesicles with an average diameter of ~104 nm. Upon NIR laser exposure, photothermal effects triggered the release of the vesicular components, and the NPs disassembled into ultrasmall fragments (~6 nm). This transformation highlighted the distinct functional roles of each size: the 104 nm vesicles were essential for stability and targeting during circulation, whereas the generated 6 nm fragments possessed the necessary diffusivity to infiltrate the deep tumor mass that was impermeable to the vesicles.[161] To further maximize deep tissue access, minimizing the final particle size to the ultrasmall scale (< 5 nm) is critical. Focusing on this dimensional

optimization, Pan et al constructed an ultrasmall NIR-responsive nanocomposite composed of amphiphilic gelatin (AG)-wrapped PAMAM dendrimers conjugated with arginine, DOX, and copper sulfide (CuS). The initial nanocomposite measured ~5 nm in diameter. Upon NIR light irradiation, the structure degraded into ultrasmall CuS NPs (~3 nm). This degradation mechanism ensured that the active therapeutic agents were released from the carrier matrix, enabling deep-tissue accumulation and enhanced chemo-photothermal therapy that would otherwise be limited by the steric hindrance of the intact nanocomposite.[162] These studies collectively demonstrate that NIR-triggered size reduction effectively bridges the gap between systemic stability and intratumoral diffusivity, allowing nanocarriers to bypass the physiological barriers of the tumor stroma.

Hypoxia-Sensitive Size-Switchable Nanoparticles

Hypoxia, a hallmark of solid tumors, presents a unique physiological trigger that can be utilized to develop intelligent, stimuli-responsive drug delivery systems.[163] Tumor sites have pO2 below 10 mmHg due to insufficient blood supply from disordered blood vessels, compared to normal tissues, which have around 40 mmHg pO2.[164] Hence, hypoxia in solid tumors elevates the expression of reductases such as nitroreductase, quinone reductase, and azoreductase, a driving force in cancer progression that promotes invasiveness, metastasis, and, critically, resistance to conventional therapies.[164] Smart nanocarriers are rationally engineered with stimulus-responsive linkages that remain stable under the oxidative conditions of systemic circulation but selectively cleave and undergo size transformation in the reductive and hypoxic TME, enabling controlled drug release and improved deep intratumoral penetration.[165] These NPs have specific chemical bonds that are selectively susceptible to these conditions; one of them is nitroaromatic compounds (eg, nitroimidazole), which are activated by cytosolic nitroreductase enzymes that are upregulated under hypoxic conditions Nitroreductase facilitates the bioreduction of the nitro group (NO_2) using cofactors such as nicotinamide adenine dinucleotide (NADH/NADPH)[164,166] Another linker is the azobenzene bond, which is reduced by azoreductase enzymes. This process involves the reductive cleavage of the AZO bond, splitting the linker into two constituent aromatic amines utilizing NADPH as a coenzyme.[166] For instance, in polymeric micelles, the Azo bond often serves as the junction linking hydrophilic blocks (eg, PEG) to hydrophobic blocks (eg, polystyrene) in an amphiphilic copolymer (eg, PEG-N=N-PS).[167]

Implementing this azobenzene-based design strategy to achieve structural adaptability, Xu et al developed a hypoxia-responsive micellar system based on azobenzene-centered block copolymers—poly(oligo(ethylene glycol) methacrylate)-block-poly(ε-caprolactone)-azobenzene-poly(ε-caprolactone)-block-poly(oligo(ethylene glycol) methacrylate) [POEGMA-b-PCL-Azo-PCL-b-POEGMA]. This amphiphilic copolymer self-assembled into spherical micelles encapsulating DOX and Ce6. Under hypoxic tumor conditions, the azobenzene moieties within the polymer backbone were reduced to aniline, altering the hydrophobic–hydrophilic balance of the micelles. This chemical transformation led to a shift in micellar morphology and resulted in a significant reduction in particle size. This structural transformation addressed a critical delivery barrier: the initial large micelles protected the payload during circulation, while the hypoxia-triggered disassembly into smaller units allowed the therapeutic agents to diffuse deeply into the poorly perfused, hypoxic core, a region typically inaccessible to larger, non-responsive nanocarriers.[130] These hypoxia-sensitive, size-transformable nanocarriers represent a promising strategy to overcome the physiological barriers associated with solid tumors. By capitalizing on the unique redox chemistry of the tumor core, such systems ensure that deep penetration occurs exactly where it is needed most, bypassing the diffusion limits that restrict conventional therapies. Table 3 presents an overview of size-switching nanocarriers along with their key physicochemical properties.

Surface-Modified Nanoparticles for Enhanced Tumor Delivery

The physical characteristics of NPs, including shape, size, and surface charge, play a pivotal role in determining their transport behavior within solid tumors.[169,170] Similar to other noncompaction systems, modifying the particles' surface with various chemical components is beneficial for extending NPs' circulation by preventing RES clearance.[171,172] Among these characteristics, surface charge has been identified as a key factor influencing cellular uptake, systemic stability, immune recognition, drug release, and penetration into tumor tissues.[173] To explore this further, Budiarta et al engineered ferritin nanocages with distinct surface charge properties. Four variants were produced: wild-type ferritin, negatively charged ferritin, positively charged ferritin, and a specifically engineered version termed negatively charged

Table 3 Summary of Size-Switching Nanocarrier Systems and Their Key Properties

No.	Structure Name	Initial Size (nm)	Final Size (nm)	Stimulus Type	Payload	Key Therapeutic Outcome	Ref.
1	JNP Ve	100	8.6	GSH-responsive	IR1061	Significant inhibition of orthotopic liver tumors via deep penetration	[74]
2	PAMAM prodrug-loaded Nanocluster	100	5	Acidic pH responsive	Cisplatin	Achieved deep penetration leading to 95% inhibition of drug-resistant tumors and 88% suppression of pancreatic tumors	[67]
3	MPNs	170	< 20	pH-responsive (acidic)	Doxorubicin	Superior suppression of large 4T1 tumors (~250 mm^3) with reduced systemic toxicity	[75]
4	SPN	170	< 20	pH- and Redox-responsive	Camptothecin	Achieved ~92.1% tumor inhibition in breast cancer with deep penetration (>200 μm) and real-time MRI monitoring	[140]
5	DMA-NPs	170	–	Acidic pH responsive Redox-responsive	Podophyllotoxin	Achieved 94.2% inhibition of multidrug-resistant lung tumors via deep penetration	[141]
6	^{DA}T-PPED&F	180	100	pH-responsive (acidic)	Doxorubicin	Achieved ≈98% tumor growth inhibition via magnetically actuated active deep penetration	[142]
7	PEG-Ce6 @PAEMA	103.6	12.9	pH-responsive (acidic)	Chlorin e6	Achieved 75.9% tumor growth inhibition via deep penetration and membrane-targeted photodynamic therapy	[143]
8	AuNC@CBSA-ICG@HA	200	50	Hyaluronidase-responsive	ICG	Achieved 95.0% tumor growth inhibition in breast cancer	[21,168]
9	DGL-GA-CDA-DOX-HA	182.5	47.7	Hyaluronidase-responsive	Doxorubicin	Achieved 71.6% tumor inhibition in hepatocellular carcinoma	[147]
10	PEG-PPS Micelles	150	70	ROS-responsive	Fe3O4, HC	Achieved significant tumor inhibition	[151]
11	RLPA-NPs	–	–	pH- and ROS-responsive	Paclitaxel, β-Lapachone	Achieved 90.4% tumor inhibition and suppressed lung metastasis	[152]
12	p(AAm-co-AN) -g-PEG-LA/AuNRs	101	7	NIR-responsive	Doxorubicin	Achieved 91.9% tumor inhibition	[79]
13	PTX/PDA@M-C6	104	6	NIR-responsive	Paclitaxel	Achieved 96.8% tumor inhibition	[161]
14	AG-PAMAM-CuS-DOX	5	3	NIR-responsive	Doxorubicin	97.0% tumor inhibition	[162]
15	POEGMA-b-PCL-Azo-PCL -b-POEGMA	100-150	–	Hypoxia-responsive	Doxorubicin, Chlorin e6	94.6% tumor inhibition via hypoxia-triggered deep penetration	[130]

Abbreviations: MMP 2, Matrix metalloproteinase 9; GSH, glutathione; ROS, reactive oxygen species; PAMAM, poly amidoamine; JNP, Janus NP; SPN, stimuli-responsive poly pro-drug NPs; PEMA, poly(2-azepane ethyl methacrylate); BSA, bovine serum albumin; ICG, indocyanine green; DGL-GA-CDA-DOX-HA, poly-L-lysine@glycyrrhetinic acid@cyclohexane dicarboxylic anhydride@doxorubicin@ HA; PPS, poly propylene sulfide; p(AAm-co-AN)-g-PEG-LA, Poly acrylamide-acrylonitrile-polyethylene glycol-lipoic acid; PDA, polydopamine; PTX, paclitaxel; HBPTK-Ce6, hyperbranched polyphosphoester containing thioketal units and chlorin e6; POEGMA-b-PCL-Azo-PCL -b-POEGMA, azobenzene-centered copolymers poly oligo (ethylene glycol) methacrylate-block-poly(ε-caprolactone)-azobenzene-poly(ε-caprolactone)-block-poly oligo (ethylene glycol); HSA, human serum albumin; MPNs, multi-pocket NPs; HC, Hypocrellin.

ferritin-1C. The wild-type, composed of 24 subunits forming a hollow protein shell, served as the neutral control. The negatively charged variant was generated by substituting four amino acids per subunit with glutamic acid. In comparison, the positively charged variant was developed by replacing nine amino acids per subunit with lysine or arginine. To optimize drug loading, the negatively charged ferritin-1C included a single cysteine residue (K53C) per subunit, enabling site-specific conjugation of DOX via maleimide chemistry. This modification significantly improved drug loading efficiency while reducing nonspecific interactions. Experimental results showed that the negatively charged variant

https://doi.org/10.2147/IJN.S563233

exhibited the highest DOX encapsulation efficiency, significant uptake by macrophage cells, and measurable cytotoxicity in MCF-7 breast cancer cells.[174] While optimizing static surface properties, such as charge, is essential, incorporating dynamic, stimuli-responsive surface modifications offers superior control over drug release. To achieve this through light-triggered conformational changes, Yao et al designed azobenzene-functionalized interfacial cross-linked reverse micelles (AICRMs) capable of light-triggered conformational switching. These NPs, loaded with 5-fluorouracil (5-FU), incorporated azobenzene groups that transform from a polar cis conformation to a nonpolar trans conformation upon exposure to 530 nm light. This transition led to NP aggregation and the subsequent release of 5-FU. The rapid drug release allowed the therapeutic agent to penetrate deeply into tumor tissue before uptake by surrounding cells, resulting in a tumor inhibition rate of 86.2% in preclinical models.[175]

Another critical surface challenge is the "PEG dilemma," where PEGylation extends circulation but hinders cellular uptake. To resolve this conflict through on-demand surface remodeling (dePEGylation), Zeng et al synthesized amphiphilic metallodrug assemblies, the PEGylated Ru complex (Ru-PEG). This complex includes an anticancer Ru complex, a red-light-cleavable PEG ligand, and a fluorescent pyrene group for imaging and self-assembly. They used PEG to decrease protein adsorption and immune recognition; moreover, by using PEG, they improved the solubility of Ru, enhancing its self-assembly into vesicles. Upon first irradiation of red light, triggers dePEGylation and changes the vesicles to large compound micelles that are smaller in diameter with an average hydrodynamic diameter of about 520 nm as measured by dynamic light scattering (DLS); the second irradiation targeted the internalized large compound micelles, generating intracellular singlet oxygen ($^1O_2$) and causing the release of the enzyme cathepsin B from lysosomes into the cytoplasm, ultimately leading to cancer cell death.[176]

These studies demonstrate that rational surface modification of NPs is a powerful strategy to enhance targeted drug delivery, improve pharmacokinetics, and overcome biological barriers in cancer therapy. By tailoring surface charge, incorporating stimuli-responsive elements, or functionalizing with targeting ligands, researchers can significantly enhance tumor selectivity, cellular uptake, and therapeutic efficacy.

Ligand-Functionalized Nanoparticles for Targeted Tumor Penetration

Functionalization of NPs with targeting ligands is a powerful strategy to enhance tumor penetration and therapeutic efficacy.[177] Ligands such as aptamers, antibodies, and peptides can be conjugated to NP surfaces to selectively recognize receptors overexpressed on tumor cells, thereby improving drug accumulation and minimizing off-target effects.[178–180] This selective recognition confers homing abilities to the NPs, distinguishing them from systems that rely solely on passive accumulation via the EPR effect. Homing moieties function as "molecular addresses," enabling nanocarriers to actively navigate the complex circulatory system and specifically dock onto the tumor vasculature or malignant cells.[181] This process acts like a "biological GPS," in which high-affinity ligand-receptor interactions serve as a connector, preventing NPs from being removed by elevated IFP. Furthermore, specific homing ligands (eg, tumor-penetrating peptides) can trigger active transport mechanisms, such as endocytosis or transcytosis, thereby facilitating the extravasation of NPs deep into the avascular tumor stroma.[182]

Jin et al reported a biotin-modified polymeric liposome (ASL-BIO-MPL) that releases micelles at the tumor site. The liposome's MMP-9-sensitive outer shell degraded in response to tumor-overexpressed enzymes, liberating ~40 nm micelles capable of deep tissue infiltration. Biotin ligands mediated tumor targeting, while a follow-up avidin administration scavenged residual biotinylated carriers from normal tissues, reducing systemic toxicity. This strategy highlights how ligand selection can be combined with environmental triggers to maximize therapeutic precision.[183] Ligand-based designs also use environmental selectivity to minimize side effects. By refining the ligand-receptor interaction to respond to microenvironmental signals, Liu et al developed pH-dependent anti-EGFR antibodies that preferentially bound EGFR in acidic TMEs,[184] thereby enhancing tumor accumulation while avoiding normal tissues. Combining ligand targeting with external physical triggers to boost penetration further, Xiong et al created a cRGD-modified, NIR-triggered liposomal platform (PAM/Pt@IcLipo).[185] The cRGD peptide specifically targeted αvβ3 integrins overexpressed in tumor vasculature, while NIR irradiation induced a size reduction from 162 nm to 8.6 nm, enabling deeper tumor penetration and efficient drug release. While single-ligand systems are effective, employing dual-targeting strategies can further enhance specificity and cellular internalization. Adopting this multi-ligand approach, Yang et al developed an exosome-based multifunctional platform (CDs: Gd, Dy-TAT@Exo-RGD) combining two targeting ligands. RGD peptides mediated integrin-specific tumor accumulation, and TAT peptides promoted

nuclear delivery. Encapsulation within macrophage-derived exosomes further enhanced tumor homing and biocompatibility, while the system also provided dual imaging capabilities for photothermal therapy and MR/CT imaging (Figure 5).[186] Transitioning from passive circulation to active, controlled navigation, Andhari et al developed a magnetically guided nanobot system for targeted DOX delivery. This system utilized magnetic Fe_3O_4 NPs conjugated with anti-epithelial cell adhesion molecule (EpCAM) monoclonal antibodies, which were attached to multi-walled carbon nanotubes (MWCNTs) loaded with DOX·HCl. The carbon nanotubes were oxidized to introduce carboxylic acid groups, facilitating covalent attachment of targeting and drug-loading components. Functionalization with anti-EpCAM mAb enabled specific recognition of EpCAM-overexpressing cancer cells, enhancing selective drug delivery to malignant tissues.[184] Finally, to extend ligand-mediated targeting to intraoperative surgical navigation, Krishnan et al developed an NIR fluorescent nanoprobe for real-time imaging and surgical navigation in prostate cancer. The platform employed prostate-specific membrane antigen (PSMA)-targeted quantum dots (PSMA-QD655), which offer deep tissue imaging capability. The quantum dots were initially PEGylated to

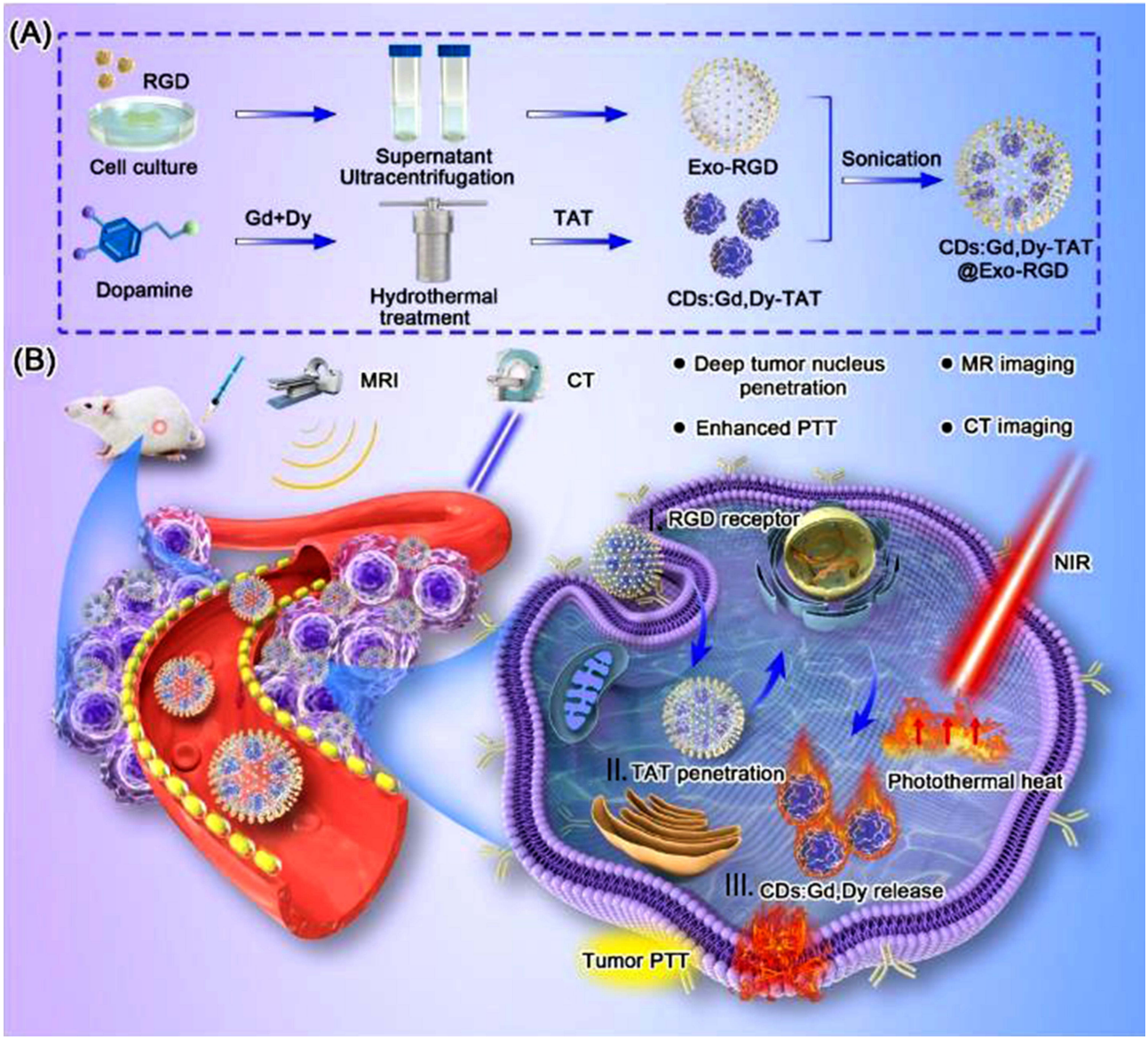

Figure 5 Design and mechanism of the multifunctional CDs:Gd,Dy-TAT@Exo-RGD nanoplatform. (**A**) Schematic synthesis process: RGD-modified exosomes (Exo-RGD) are obtained from cell culture supernatant through ultracentrifugation and combined with carbon dots doped with Gd and Dy (CDs:Gd,Dy-TAT) via sonication to produce CDs:Gd,Dy-TAT@Exo-RGD. (**B**) Therapeutic and diagnostic functions in TME: The nanoplatform targets tumor sites through RGD-integrin interactions, penetrates deeply into tumor nuclei via TAT peptides, and releases CDs:Gd,Dy under NIR irradiation, generating photothermal heat for enhanced photothermal therapy. Additionally, the Gd and Dy components enable dual-modality MR/CT imaging for precise tumor diagnosis. Adapted with permission from.[186]

https://doi.org/10.2147/IJN.S563233

improve aqueous stability and prolong systemic circulation. Subsequently, a heterobifunctional crosslinker, 4-maleimidobutyric acid N-succinimidyl ester, was used to conjugate DUPA, a ligand that specifically binds to PSMA. This design enhanced targeting efficiency and allowed for precise intraoperative visualization of prostate tumors.[187] These studies demonstrate that ligand-functionalized NPs, through specific receptor interactions and synergistic design features, effectively overcome biological barriers to cancer therapy. By combining receptor targeting with mechanisms such as enzyme sensitivity, pH selectivity, and size-switching, these systems achieve enhanced tumor accumulation, deep penetration, and superior therapeutic outcomes, marking a crucial step toward next-generation nanomedicines.

Rational Design of Nanoparticle Shape for Improved Tumor Penetration

Beyond surface properties, NP shape is a crucial physicochemical parameter that significantly influences their in vivo performance.[188] NP shape affects circulation time, biodistribution, and cellular uptake, ultimately determining the efficiency of drug delivery to tumor sites.[189] Different geometries interact uniquely with biological barriers, influencing their ability to avoid immune clearance, penetrate tissues, and remain at the target site. For example, specific shapes may resist aggregation in biological fluids, while others exhibit improved retention but limited circulation stability.[190,191] Yu et al demonstrated that shape control directly impacts NP behavior in tumors. They found that while nanofibers showed superior retention within tumor tissues compared to spherical NPs, their elongated form compromised stability in the bloodstream, limiting overall therapeutic efficacy. This finding highlights the need for shape-adaptable systems that can balance both circulation and tumor retention.[21] Responding to this need for adaptive geometry to reconcile the "circulation-retention paradox, Jia et al developed a shape-transformable, charge-reversible NP (DHP@BPP) for combined photodynamic immunotherapy and chemotherapy. These NPs remain spherical during circulation, ensuring stability and prolonged systemic exposure. Upon encountering the TME, MMP-2 triggers proline cleavage, altering hydrophilic–hydrophobic interactions and driving a shape transformation from spheres to nanofibers. This transformation enhances cellular uptake, tumor retention, and penetration, ultimately improving therapeutic outcomes. The dual mechanism, charge reversal and shape adaptability, enables precise drug delivery while maximizing antitumor efficacy.[129] While enzyme-responsiveness is effective, integrating biomimetic features with alternative triggers, such as ROS, can further enhance immune evasion and targeting. Advancing this bio-inspired direction, Liu et al synthesized a macrophage-mimicking shape-changing nanomedicine (I-P@NPs@M) for multifunctional breast cancer therapy. Initially designed as spherical micelles, these NPs undergo a ROS-induced transformation into elongated nanofibers upon tumor irradiation. This morphological switch prolongs drug retention at the tumor site and improves cellular internalization. Furthermore, the elongated fibers allow sustained drug release, enhancing the potency of combined PDT and chemotherapy. The ROS generated not only drives the shape transition but also directly kills tumor cells and activates prodrugs, thereby amplifying therapeutic effects.[128] These studies underscore the importance of shape engineering as a next-generation strategy in nanomedicine. Unlike static spherical carriers, shape-transformable NPs intelligently adapt to the TME, maintaining circulation stability while achieving deep tissue penetration and prolonged drug activity. By coupling shape dynamics with other design elements, such as charge reversal, ROS-responsiveness, and biomimicry, researchers are unlocking new possibilities for precision cancer therapy that overcome the limitations of conventional drug delivery systems.

In silico Approaches and Artificial Intelligence in Nanoparticle Design and Optimization

The rational development of nanomedicines depends on fine-tuning multiple physicochemical parameters, such as particle size, surface chemistry, shape, and ligand functionalization, to achieve optimal therapeutic performance.[192,193] Traditionally, the design, screening, and optimization of NPs have relied heavily on experimental approaches, which are both time-consuming and resource-intensive.[194] In recent years, in silico methodologies have emerged as powerful tools to overcome these limitations. Among these, artificial intelligence (AI), machine learning (ML), and molecular dynamics (MD) simulations have played pivotal roles in accelerating NP discovery, enabling researchers to predict biological behavior, optimize formulations, and reduce the need for extensive in vivo testing (Figure 6).

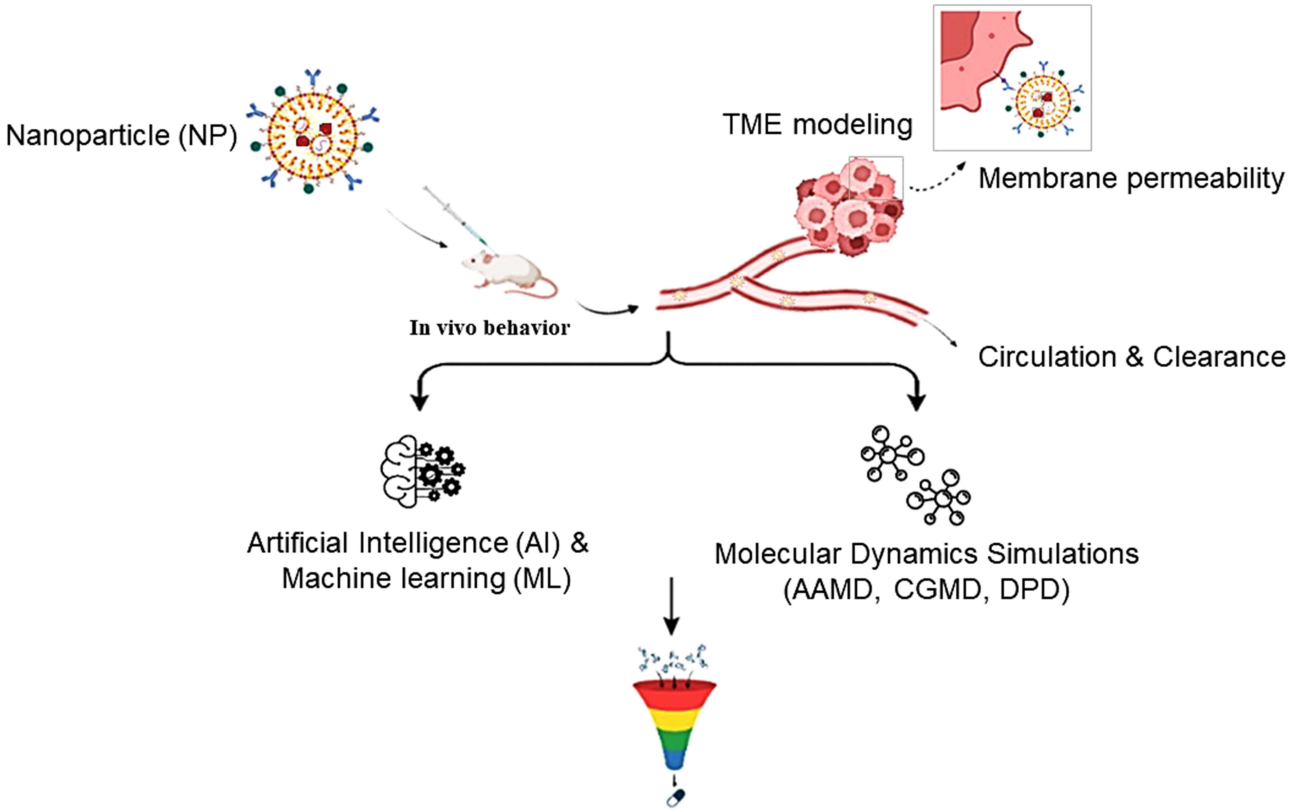

Figure 6 Schematic of in silico approaches (AI/ML and molecular dynamics simulations) used to relate nanoparticle physicochemical properties to optimized nanoparticle design, drug delivery performance, tumor targeting, PBPK prediction, and toxicity assessment.

Artificial Intelligence and Machine Learning in Nanoparticle Optimization

AI and ML techniques have changed how NPs are designed and improved, enabling the analysis of large, complex datasets that traditional statistical methods cannot handle.[195,196] These computational methods can accurately predict NP-cell interactions, drug delivery efficiency, and pharmacokinetic properties using minimal input data, such as particle size, surface chemistry, and tumor model characteristics.[197] Lin et al conducted a significant study in this domain, using deep neural networks (DNNs) on data from the Nano-Tumor Database to identify patterns that enable precise predictions of delivery efficiency across various NP formulations and cancer types. This model surpassed other machine learning models, including linear regression, random forests, support vector machines (SVMs), and bagged models.[198] Expanding the predictive scope from general delivery efficiency to specific organ accumulation patterns, Mahdi et al used several ML algorithms, including Kernel Ridge Regression (KRR), Bayesian Ridge Regression (BRR), and K-Nearest Neighbors (KNN), to investigate NP biodistribution patterns in major organs. This showed that ML models, especially KRR, can accurately classify and measure NP accumulation even across highly diverse biological systems.[199] Moving beyond physicochemical parameters to the structural analysis of the biological barriers themselves, Zhu et al developed nano-ISML. This image-segmentation machine learning method analyzed more than 67,000 blood vessels across 32 tumor models. This method revealed significant variability in vascular permeability (exceeding 100-fold differences) and identified unique transport mechanisms, facilitating the strategic design of protein NPs tailored to various vessel types.[200] Representing a paradigm shift from static prediction to autonomous, real-time experimental optimization, Ortiz-Perez et al used a unified platform that combined microfluidics, high-content imaging, and active machine learning to design PLGA-PEG NPs to improve their uptake by MDA-MB-468 human breast cancer cells. This closed-loop system achieved a significant enhancement, increasing cellular uptake from 5-fold to 15-fold in just two machine-learning-guided iterations over two weeks. This shows that a data-driven approach can speed up the development of nanomedicine.[201] Furthermore, integrating ML with physiologically based pharmacokinetic (PBPK) modeling enables

https://doi.org/10.2147/IJN.S563233

simulation of the absorption, distribution, metabolism, and excretion (ADME) profiles of NPs in tumor environments.[198] This kind of predictive modeling not only accelerates the search for effective formulations but also facilitates the design of nanomedicines with greater clinical translation potential. A concise overview of the major AI/ML models used in tumor-targeted NP optimization is summarized in Table 4.

To move nanomedicine forward, we need to understand the complex interactions at the nano-bio interface. Multi-omics approaches that combine genomics, proteomics, metabolomics, and high-resolution imaging are the best way to simplify this complexity. These technologies enable systematic study of NP uptake, intracellular fate, and tissue spatial distribution. They also show how cells respond to NPs at the single-cell level. The real power comes from putting together these different types of data. For example, linking CT or MRI data with genomic profiles can help identify biomarkers that predict the effectiveness of nanomedicine. Artificial intelligence, especially bioinformatics algorithms and graph neural networks (GNNs), is crucial for assembling these large, multimodal datasets. GNNs, such as scMoGNN, can build unified networks that leverage biological knowledge across different omics layers. This allows them to model higher-order relationships among the properties of NPs, cell features, and the microenvironment. This combined analysis enables data-driven customization of NPs, enabling them to be designed to elicit specific cellular responses and to select the ideal, most personalized drug delivery platforms based on a patient's multi-omic profile. To fully realize the potential of multi-omics for guiding the rational design of next-generation nanotherapeutics, it is crucial

Table 4 AI/ML Approaches Used in Nanoparticle Design, Prediction, and Optimization

No.	Method	Predictive Algorithms	Inputs	Output Targets	Ref.
1	Supervised ML	Random Forest (RF), Support Vector Machine (SVM), Gradient Boosting (XGBoost/LightGBM), K-nearest neighbors (K-NN)	NP physicochemical properties (size, zeta potential, shape, type surface chemistry), in vitro efficacy data, and in vivo Pharmacokinetics and Biodistribution (PK/BD) measurements (Nano-Tumor Database)	Prediction of penetration and tumor delivery efficiency, cytotoxicity, and organ biodistribution	[198,202,203]
2	Deep Neural Networks (DNNs)	Multi-layer perceptrons, feedforward networks (FNNs), Autoencoders, feature embeddings	NP physicochemical properties, microscopy images, molecular sequences, and spectral data	Novel NP designs, prediction of delivery efficiency, toxicity, drug release profiles, and interaction predictions	[198,204,205]
3	Convolutional Neural Networks (CNNs)	U-Net, 2D/3D CNNs, encoder-decoder architecture	Confocal 3D microscopy images, histology data, and tomographic scans	Prediction of penetration depth, Automated segmentation, and spatial concentration maps	[206,207]
4	Graph Neural Networks (GNNs)	GCN, GAT, SchNet, message-passing neural nets (MPNN)	Structural graphs for NP components, particle morphology graphs	Predict particle properties, effective interactions with membranes	[208–210]
5	Bayesian optimization	Bayesian optimization, Gaussian Process Regression (GPR)	Minimum experimental datasets, formulation variables, process conditions	Optimize formulation parameters, advance experimental searches for desired NP properties	[211–213]
6	Reinforcement learning (RL)	Deep Q-Networks (DQN), policy gradients RL	Sequential synthesis data, iterative formulation experiments	Optimization of NP formulation parameters	[214]
7	Multi-omics integration	Random Forest, multimodal deep neural networks	Genomics, proteomics, transcriptomics, and imaging datasets	Personalized medicine, patient stratification for NP therapy	[215]

to overcome challenges, such as the need for substantial computing power and robust NP labeling methods (eg, DNA barcoding).[216–223]

Computational Modeling of Nanoparticle–Membrane Interactions

In parallel with AI-based approaches, molecular simulations offer critical mechanistic insights into the interactions between NPs and biological membranes, a key determinant of cellular uptake, biodistribution, and therapeutic efficacy[192,224,225] These simulations vary in their resolution and computational demand, providing complementary perspectives at different scales. At the most detailed level, all-atom MD (AAMD) captures atomic-scale interactions, enabling precise characterization of NP binding, conformational changes, and perturbations in the lipid bilayer.[198] For larger systems or longer timeframes, coarse-grained molecular dynamics (CGMD) simplifies atomic representations by grouping atoms into beads, reducing computational complexity while preserving essential physicochemical properties.[226] This approach is beneficial for exploring the collective behavior of NPs and membranes over extended periods. At an even higher level of simplification, dissipative particle dynamics (DPD) employs a highly coarse-grained model to efficiently simulate mesoscale processes, including NP wrapping, membrane deformation, and endocytosis.[197,227] Demonstrating the utility of this mesoscopic approach for analyzing complex tissue barriers, Kang et al used DPD to simulate, at a mesoscopic level, how Laminin-332-functionalized solid lipid NPs (SLNLam) interact with each other and with the lipid membrane. The goal was to understand how physical and chemical factors, such as adhesion, membrane fusion, and interparticle forces, affect skin penetration.[194] Using CGMD, Dondani et al demonstrated that polymer coatings strongly influence membrane interactions: PEGylated NPs displayed weak binding, whereas those with mixed hydrophobic/hydrophilic coatings showed enhanced retention.[228] Complementary AAMD studies confirmed these findings at the atomic scale, providing detailed insights into polymer–membrane dynamics. Finally, at the highest level of resolution, atomic details govern how different core materials interact with lipid bilayers. Employing AAMD to investigate these fundamental material-specific properties, Singhal et al employed AAMD to examine how NP size and composition affect membrane interactions.[224] Their simulations revealed that silver (Ag) NPs exhibit strong binding and penetrate the hydrophobic core of membranes, especially at larger sizes (3–5 nm), whereas titanium dioxide (TiO_2) showed minimal interaction, and silica (SiO_2) localized primarily at the bilayer–water interface. These observations highlight the critical roles of size, surface chemistry, and material properties in governing NP behavior at biological interfaces.

In silico approaches, ranging from AI-driven predictive modeling to multiscale molecular simulations, are revolutionizing the field of nanomedicine. While AI and ML enable high-throughput screening and optimization of NP formulations, molecular simulations provide mechanistic insights into their interactions with biological systems. The synergy of these methods accelerates the rational design of NPs, reduces reliance on costly experimental trials, and opens new avenues for the development of next-generation precision nanotherapeutics.

Emerging Experimental Platforms for Evaluating Tumor Penetration

Cell culture is an important in vitro tool that has helped us learn a lot about cellular mechanisms, tissue architecture, disease pathogenesis, and pharmacological effects. Most cancer research studies have used two-dimensional (2D) monolayer cultures. However, these traditional models have some inherent problems, such as abnormal growth patterns, changes in cell shape and polarity, and disrupted interactions between cells and the extracellular matrix. Because of these major drawbacks, researchers have developed increasingly advanced experimental platforms that more closely mimic in vivo physiological conditions.[229–231] Among these, three-dimensional (3D) culture systems including tumor spheroids, organoids, and microfluidic tumor-on-a-chip devices have emerged as a promising alternative that recapitulate key physical and biological constraints present in solid tumors such as gradients of oxygen and nutrients, complex cell-cell interactions, heterogeneous ECM density and composition, elevated IFP, functional endothelial barriers with leakage and also facilitate developing targeted therapeutic strategies.[232–235] This section outlines the key advantages of these experimental systems, highlighting specific studies that have employed them to analyze NP transport and to validate corresponding computational forecasts.

Spheroids

Spheroids are three-dimensional aggregates of cancer cells organized into spherical shapes that form spontaneously without the need for an unnatural substrate. These models naturally recreate key microenvironmental conditions that regulate fundamental cellular processes. When spheroids are larger than 500 μm, they show metabolic gradients and resemble non-vascularized or weakly vascularized tumors. An outer layer of proliferating cells, a middle layer of quiescent cells, and an inner layer of hypoxic and necrotic cells make up the multilayered structure.[236,237] Physiological gradients provide resistance to chemotherapy and radiation, as observed clinically, rendering spheroids a pertinent model for investigating microenvironment-induced therapeutic responses.[238,239] Several spheroid models have been created based on their cellular origin. Multicellular tumor spheroids (MCTS), usually obtained from cancer cell lines, are easy to reproduce, readily expand to large-scale cultures, and well-suited to high-throughput screening platforms. Even though they lack the full histological complexity of primary tumors, MCTS perform well at recreating clinically relevant biochemical gradients and resistance patterns.[240,241] On the other hand, tumor spheroids generated from enzymatically or mechanically detached patient tumor tissue keep their natural genetic and cellular diversity. When grown in serum-free conditions with added growth factors, these spheroids often contain more cancer stem-like cells, making them a better model of how tumors behave in patients. Spheroids remain among the easiest and most useful 3D tumor models. They allow researchers to study early tumor architecture, NP and drug penetration, cellular invasion and migration, and treatment responses in a setting more like the in vivo TME.[242–244]

Using this heterogeneous architecture to visualize nanocarrier transport, Pratiwi et al studied mesoporous silica NPs (MSNs) of various surface chemistries and sizes in MG-63 spheroids using two-photon microscopy. They employed hierarchical clustering analysis (HCA) to investigate the physicochemical properties and the relationship between penetration and profile of MSNs in a spheroid model. They showed that the size and surface charge of NPs uniquely influence their transport, and that MSNs' stability determines their ability to reach the hypoxic region.[245] While imaging reveals distribution patterns, extracting precise transport parameters requires integrating experimental data with mathematical modeling. Bridging these domains, Nagesetti et al combined silica NP penetration experiments in SKOV-3 spheroids with a Bayesian inverse estimation method to infer cell uptake rates, then embedded these parameters with finite-element (FEM) modeling to evaluate the impact of PEG functionalization and mild hyperthermia on silica NP penetration. Their simulations, along with experimental results, showed that Carboxy-PEG-silane (cPEGSi) NPs exhibit greater uptake than methoxy-PEG-silane (mPEGSi) NPs. Also, they found that hyperthermia reduces ECM viscosity and enhances the penetration of cPEGSi NPs.[246] To further standardize the quantification of these kinetic processes without relying on complex simulations, Ahmed-Cox et al developed the Determination of Nanoparticle Uptake in Tumor Spheroids (DONUTS) in situ imaging analysis platform. This platform is a MATLAB-based pipeline that converts live confocal z-stacks of NP-treated spheroids into spatial and temporal radial uptake profiles. In this research, they found that spheroid properties, such as cell origin, density, and cell stiffness, influence NP uptake, and that smaller NPs penetrate more deeply.[247] Despite advances in 3D tumor models, extracting cell-type-specific drug responses at single-cell resolution remains challenging. To tackle this issue, Vitacolonna et al introduced a comprehensive 3D, whole-mount pipeline that integrates tissue clearing, immunostaining, confocal microscopy, and a CNN-based nuclei segmentation to quantify cell-type-specific drug responses at the single-cell level in KP4 cancer-CCD-1137Sk fibroblast co-cultured spheroids. They discovered that co-culture with fibroblasts can alter drug responses, with KP4 cancer cells frequently exhibiting greater drug sensitivity than fibroblasts. Additionally, the core regions of treated co-culture spheroids demonstrated decreased proliferation, whereas the outer regions exhibited increased apoptosis and necrosis. The research also showed that it is compatible with current AI segmentation tools and offered a batch-friendly software solution for 3D analysis. It also showed that ECM (especially collagen-1) and the microenvironment affect drug distribution and efficacy.[206]

Organoids

Organoids are another type of 3D tumor model that can differentiate and organize themselves. They are similar to the original tissue in both genetic and histological ways, and they have some advantages over traditional 2D and animal models.[242,248] Creating a robust model of tumor heterogeneity is essential for understanding how tumors function and for

developing effective treatments. Tumor organoids can retain the original tumor heterogeneity and are frequently utilized to imitate the cancer microenvironment when cultivated with fibroblasts and immune cells. They can also be used to model the physical barriers that NPs face in biological tissues. Many studies have found that tumor organoid responses to various medicines correlate well with patient responses. Tumor organoids have significant preclinical research potential due to their consistent responses and individualized characteristics.[249–252] These models can be cultured from tiny amounts of tissue or typically from adult stem cells, embryonic stem cells (ESCs), and hPSCs.[251,253] Organoids derived from PSCs are of different types and can contribute to organ failure or dysfunction.[251,253] Organoids offer many benefits, including the study of toxicity, infectious diseases, and hereditary diseases, as well as the provision of personalized medicine for each patient.[254] The absence of vasculature in organoids, however, influences their growth and maturation, resulting in behavioral differences relative to the original tissue.[255]

While organoids offer superior biological relevance, assessing their viability often requires destructive endpoint assays that prevent longitudinal monitoring. To overcome this limitation, Spiller et al developed an image-based high-content screening workflow that employs computer vision and a supervised ML linear classifier to assess drug responses in patient-derived colorectal cancer organoids (PDOs) over time. This method enables them to track each organoid and to detect patient-specific morphological signatures related to viability and treatment responses, without using fluorescent dyes. They further strengthened their research by designing a web-based visualization tool (Organoizer) to analyze intricate multivariate data.[256] Advancing the computational sophistication from standard machine learning to deep learning, and extending the application to complex tumor-immune co-cultures, Ferreira et al recently introduced OrganoIDNet, a deep-learning imaging tool designed to quantify real-time therapeutic responses in PDAC organoid cultures or organoid-peripheral blood mononuclear cells (PBMC) co-cultures through the analysis of time-resolved bright-field images. The study exhibited size-specific drug responses to gemcitabine and immunotherapy with Atezolizumab, as confirmed by CellTiter-Glo proliferation endpoint measurements. It demonstrated that live imaging, when analyzed with OrganoIDNet, can uncover precise treatment effects that endpoint assays may miss.[257]

Microfluidic Tumor-on-Chip Systems

The TME possesses unique human biochemical and biophysical properties that are challenging to recreate in typical 2D cell cultures or animal models.[258] These limitations hinder the translational efficacy of anticancer strategies, as conventional systems inadequately represent critical characteristics, including tissue-tissue interfaces, interstitial flow, ECM composition, mechanical signals, and cellular heterogeneity. Consequently, there is increasing demand for sophisticated in vitro platforms that more accurately emulate human tumor physiology and link preclinical findings to clinical outcomes.[259–262]

Microfluidic organ-on-a-chip technology has emerged as a promising solution, integrating 3D cell culture, microengineering, and controlled fluidic environments to recreate physiologically relevant tissue functions.[263–267] Organ-on-a-chip devices allow for precise control of shear stress, nutrient and oxygen gradients, barrier permeability, and drug exposure profiles. They also offer benefits such as lower experimental costs, higher throughput, greater reproducibility, and reduced need for animal testing.[268–270] Tumor-on-a-chip systems build on this technology by adding cancer-specific architectural and microenvironmental features, such as multicellular organization, stromal components, ECM density, vascular-like channels, and dynamic biochemical signaling.[271,272]

Tumor-on-a-chip models allow real-time examination of key cancer processes, including tumor growth, invasion, intravasation, immune interactions, metastasis, drug penetration, treatment response prediction, and toxicity profiling.[253,270] These platforms better illustrate the complexity of the TME than static 3D cultures, as they partially reconstruct the native tumor architecture, including cell-cell communication, matrix organization, vascular mimicry, and physical stresses. As a result, tumor-on-a-chip technology is a useful translational tool that could accelerate preclinical testing, improve personalized therapeutic testing, and help with precision oncology applications.[260,273–275] In a recent study, Moerdler et al introduced PTOLEMI, a Python-based image analysis framework that uses machine learning to automate the high-throughput evaluation of microfluidic tumor assays. The system combines a Faster R-CNN-based detection architecture with an artificial neural network (ANN) to identify and categorize live and dead cells quickly, as well as different cell types, in complex biopsy-derived samples. PTOLEMI significantly shortens analytical time

compared to manual evaluation and other deep learning models like CNNs, RNNs, U-Nets, DenseNets, and transfer learning. It performs this by achieving about 96% accuracy and processing large image sets in seconds. This platform demonstrated how AI-assisted microfluidic systems can simplify drug-response measurements, make tumor-on-a-chip experiments easier to understand, and support rapid, clinically actionable decision-making in personalized oncology.[276] Additionally, current viability assays for 3D cancer spheroids used in high-throughput microfluidic drug screening are often unreliable and destructive. To tackle this problem, Chiang et al designed a label-free, non-destructive viability estimation model that uses phase-contrast images to predict spheroid survival without fluorescent labeling. The framework allowed for continuous monitoring of drug response and was strongly correlated with standard LIVE/DEAD staining. It used a microfluidic chip capable of producing about 12,000 spheroids per device. It demonstrated promising generalizability to novel drugs and cell lines, as well as transferability across different laboratory microscopes. Overall, this work illustrated how integrating deep learning with microfluidic spheroid systems can be a widely applicable tool for accelerated drug screening and improve the scalability and reproducibility of preclinical testing.[277] Furthermore, Deng et al recently employed a microfluidic tumor-on-a-chip system to examine the impact of the microstructure of single-chain polymeric NPs (SCPNs) on their penetration, uptake, and conformational stability in three-dimensional tumor environments. The platform incorporates MCF-7 spheroids within a Matrigel/collagen–hyaluronic acid ECM, facilitating accurate evaluation of NP dynamics during ECM penetration and cellular uptake. While all tested SCPNs efficiently penetrated the ECM, their cellular uptake and conformational stability were highly dependent on their polymer microstructure. Glucose-based SCPNs achieved the highest cellular uptake, while charged NPs adopted more open conformations compared to hydrogen-bond-stabilized SCPNs, which retained compact folded structures. This study highlights the utility of tumor-on-a-chip platforms for elucidating structure-function relationships in polymeric nanocarriers and for giving important information about how to design NPs for targeted therapeutic applications.[278]

Limitations and Future Prospects

Despite significant progress in the development of nanoparticle delivery systems, the translation from bench to bedside remains slow. A primary obstacle is the inherent complexity and heterogeneity of the TME. While strategies such as size-switching and surface modification have shown promise, a critical evaluation reveals several limitations that must be addressed.

Although programmed delivery systems that respond to pH or enzymes demonstrate efficacy in mouse models, clinical translation is hindered by inter- and intra-patient variability. For instance, the pH gradient in human tumors is often less distinct than in controlled heterologous models, potentially leading to off-target disassembly or failure to trigger size reduction. Furthermore, the synthesis of these complex, multi-component nanocarriers (eg, multi-stage size-switchable systems) presents significant manufacturing challenges. Scale-up reproducibility and long-term stability remain major hurdles often overlooked in proof-of-concept studies.

In the field of ligand-functionalized NPs, a critical paradox exists known as the “binding site barrier.” While high-affinity ligands (eg, antibodies) are designed to enhance uptake, comparative analyses suggest they may hinder deep penetration by binding irreversibly to the first layer of perivascular tumor cells. This creates a peripheral “barrier” that prevents the drug from diffusing to the tumor core. Future designs must optimize ligand affinity to balance binding retention and diffusive penetration, rather than maximizing binding strength alone.

Current preclinical evaluation methods also present a significant gap. Traditional 2D cell cultures fail to overcome the physical constraints of the TME, such as IFP and stromal density. Moreover, most successful deep-penetration strategies are reported in rapidly growing mouse tumors, which are often more permeable than the desmoplastic stroma of human cancers. This disconsistency necessitates a shift toward advanced in vitro platforms, such as microfluidic tumor-on-a-chip systems and patient-derived organoids, to predict clinical transport kinetics better.

To overcome current hurdles, future research must move beyond single-stimulus designs to multi-responsive systems capable of adapting to the heterogeneity of the TME. Enhancing penetration will likely require a combinatorial approach that not only optimizes the nanocarrier but also actively modulates the TME itself (eg, vascular normalization or enzymatic ECM degradation). Coupling these strategies with AI-driven design and multi-omics data will enable the development of personalized nanomedicines tailored to specific tumor profiles, bridging the gap between preclinical innovation and clinical reality.

Conclusion

Deep penetration of NPs into solid tumors remains a significant challenge due to the complex and heterogeneous TME, characterized by dense ECM, elevated IFP, stromal barriers, and abnormal vasculature. These factors collectively restrict intratumoral transport and limit the therapeutic efficacy of nanomedicines. Recent progress highlights stimuli-responsive nanocarriers as a promising strategy to overcome these barriers by exploiting tumor-specific cues such as acidic pH, enzymatic activity (eg, hyaluronidase and matrix metalloproteinases), hypoxia, and reactive oxygen species. Through programmed physicochemical transformations, including size switching, shape modulation, and surface charge reversal, these systems address the trade-off between prolonged systemic circulation and deep tumor retention. Surface engineering approaches, such as ligand-mediated targeting and charge optimization, further enhance tumor specificity and cellular uptake, underscoring the need for coordinated optimization of multiple NP properties rather than reliance on a single design parameter.

A critical advancement in this field is the integration of predictive computational tools with physiologically relevant experimental models. Artificial intelligence and machine learning enable rational NP design by predicting biological interactions and optimizing physicochemical features before synthesis. Concurrently, validation is shifting from conventional two-dimensional cultures to three-dimensional platforms, including organoids, spheroids, and tumor-on-a-chip systems, which more accurately recapitulate the physical and biological constraints of the TME. Future research should prioritize multi-stimuli-responsive systems capable of adapting to the spatial and temporal heterogeneity of tumors. Overall, effective intratumoral NP delivery will depend on the coordinated integration of smart nanocarrier design, TME modulation, advanced experimental models, and predictive computational approaches to improve therapeutic efficacy and clinical translatability.

Acknowledgment

S. M-J sincerely appreciates the financial support from the Pharmaceutical Sciences Research Center at Mazandaran University of Medical Sciences.

Disclosure

The authors report no conflicts of interest in this work.

References

1. Nazari A, Osati P, Far NP, et al. Prostate cancer and tumor microenvironment. In: *Prostate Cancer: Molecular Events and Therapeutic Modalities*. Springer; 2024:203–219.
2. Sang M, Feng L, Dong A, et al. The genomic physics of tumor-microenvironment crosstalk. *Phys Rep*. 2023;1029:1–51. doi:10.1016/j.physrep.2023.07.006
3. Jung S, et al. Advances in 3D vascularized tumor-on-a-chip technology. *Adv Exp Med Biol*. 2022;1379:231–256.
4. Chen M, Chen B, Ge X, et al. Targeted nanodrugs to destroy the tumor extracellular matrix barrier for improving drug delivery and cancer therapeutic efficacy. *Mol Pharm*. 2023;20(5):2389–2401. doi:10.1021/acs.molpharmaceut.2c00947
5. Lau R, Yu L, Roumeliotis TI, et al. Unbiased differential proteomic profiling between cancer-associated fibroblasts and cancer cell lines. *J Proteomics*. 2023;288:104973. doi:10.1016/j.jprot.2023.104973
6. Singh M, Ma R, Zhu L. Theoretical evaluation of enhanced gold nanoparticle delivery to PC3 tumors due to increased hydraulic conductivity or recovered lymphatic function after mild whole body hyperthermia. *Med Biol Eng Comput*. 2021;59(2):301–313. doi:10.1007/s11517-020-02308-4
7. Alamer M, Xu XY. The influence of tumour vasculature on fluid flow in solid tumours: a mathematical modelling study. *Biophys. Rep*. 2021;7(1):35. doi:10.52601/bpr.2021.200041
8. Chen J, Li S, Liu X, et al. Transforming growth factor-β blockade modulates tumor mechanical microenvironments for enhanced antitumor efficacy of photodynamic therapy. *Nanoscale*. 2021;13(22):9989–10001. doi:10.1039/D1NR01552D
9. Alefeld E, Haase A, Van Meenen D, et al. In vitro model of retinoblastoma derived tumor and stromal cells for tumor microenvironment (TME) studies. *Cell Death Dis*. 2024;15(12):905. doi:10.1038/s41419-024-07285-2
10. He X, Yang Y, Han Y, et al. Extracellular matrix physical properties govern the diffusion of nanoparticles in tumor microenvironment. *Proc Natl Acad Sci U S A*. 2023;120(1):e2209260120. doi:10.1073/pnas.2209260120
11. Sun Y, Chen W, Torphy RJ, et al. Blockade of the CD93 pathway normalizes tumor vasculature to facilitate drug delivery and immunotherapy. *Sci Transl Med*. 2021;13(604). doi:10.1126/scitranslmed.abc8922.
12. Awad NS, Salkho NM, Abuwatfa WH, et al. Tumor vasculature vs tumor cell targeting: understanding the latest trends in using functional nanoparticles for cancer treatment. *OpenNano*. 2023;11:100136. doi:10.1016/j.onano.2023.100136
13. Ai Y, He M-Q, Sun H, et al. Ultra-small high-entropy alloy nanoparticles: efficient nanozyme for enhancing tumor photothermal therapy. *Adv Mater*. 2023;35(23):e2302335. doi:10.1002/adma.202302335
14. Zhao N, Jiao Z, Chen L, et al. Hybrids of polysaccharides and inorganic nanoparticles: from morphological design to diverse biomedical applications. *Acc. Mater. Res*. 2023;4(12):1068–1082. doi:10.1021/accountsmr.3c00172

15. Shen X, Pan D, Gong Q, et al. Enhancing drug penetration in solid tumors via nanomedicine: evaluation models, strategies and perspectives. *Bioact Mater*. 2024;32:445–472. doi:10.1016/j.bioactmat.2023.10.017
16. Chen W, Wang W, Xie Z, et al. Size-dependent penetration of nanoparticles in tumor spheroids: a multidimensional and quantitative study of transcellular and paracellular pathways. *Small*. 2024;20(8):e2304693. doi:10.1002/smll.202304693
17. Paul P, Das S. EDL flow designing of an ionized rabinowitsch blood doped with gold and GO nanoparticles in an oblique skewed artery with slip events. *BioNanoScience*. 2023;13(4):2307–2336. doi:10.1007/s12668-023-01176-0
18. Fahes A, En Naciri A, Shoker MB, et al. Self-assembly-based integration of Ag@Au oligomers and core/shell nanoparticles on polymer chips for efficient sensing devices. *Soft Matter*. 2023;19(2):321–330. doi:10.1039/D2SM00769J
19. Roberts MG, Facca VJ, Keunen R, et al. Changing surface polyethylene glycol architecture affects elongated nanoparticle penetration into multicellular tumor spheroids. *Biomacromolecules*. 2022;23(8):3296–3307. doi:10.1021/acs.biomac.2c00386
20. Theobald N, Templeton D. A drug delivery strategy emerges that has the potential to transform cancer therapy. *Drug Discov Today*. 2024;29 (4):103923. doi:10.1016/j.drudis.2024.103923
21. Yu W, Hu C, Gao H. Intelligent size-changeable nanoparticles for enhanced tumor accumulation and deep penetration. *ACS Appl Bio Mater*. 2020;3(9):5455–5462. doi:10.1021/acsabm.0c00917
22. Mohanty RP, Liu X, Ghosh D. Electrostatic driven transport enhances penetration of positively charged peptide surfaces through tumor extracellular matrix. *Acta Biomater*. 2020;113:240–251. doi:10.1016/j.actbio.2020.04.051
23. Bishoyi AK, Nouri S, Hussen A, et al. Nanotechnology in leukemia therapy: revolutionizing targeted drug delivery and immune modulation. *Clin Exp Med*. 2025;25(1):166. doi:10.1007/s10238-025-01686-z
24. Lin J, Miao L, Zhong G, et al. Understanding the synergistic effect of physicochemical properties of nanoparticles and their cellular entry pathways. *Commun. Biol*. 2020;3(1):205. doi:10.1038/s42003-020-0917-1
25. Souri M, Golzaryan A, Soltani M. Charge-Switchable nanoparticles to enhance tumor penetration and accumulation. *Eur J Pharm Biopharm*. 2024;199:114310. doi:10.1016/j.ejpb.2024.114310
26. Salavati H, Pullens P, Ceelen W, et al. Drug transport modeling in solid tumors: a computational exploration of spatial heterogeneity of biophysical properties. *Comput Biol Med*. 2023;163:107190. doi:10.1016/j.compbiomed.2023.107190
27. Akbarishandiz S, Khani S, Maia J. Adhesion dynamics of Janus nanocarriers to endothelial cells: a dissipative particle dynamics study. *Phys Rev E*. 2024;109(6–1):064408. doi:10.1103/PhysRevE.109.064408
28. Shabbir F, Mujeeb AA, Jawed SF, et al. Simulation of transvascular transport of nanoparticles in tumor microenvironments for drug delivery applications. *Sci Rep*. 2024;14(1):1764. doi:10.1038/s41598-024-52292-0
29. Chen E, Han S, Song B, et al. Mechanism investigation of hyaluronidase-combined multistage nanoparticles for solid tumor penetration and antitumor effect. *Int J Nanomed*. 2020;15:6311–6324. doi:10.2147/IJN.S257164
30. Cho Y, Doh J. The extracellular matrix in solid tumor immunotherapy. *Trends Immunol*. 2024;45:705–714. doi:10.1016/j.it.2024.07.009
31. Zhang H, Cao X, Gui R, et al. Mesenchymal Stem/Stromal cells in solid tumor microenvironment: orchestrating NK cell remodeling and therapeutic insights. *Int Immunopharmacol*. 2024;142:113181. doi:10.1016/j.intimp.2024.113181
32. Cooley MB, Wegierak D, Exner AA. Using imaging modalities to predict nanoparticle distribution and treatment efficacy in solid tumors: the growing role of ultrasound. *Wiley Interdiscip. Rev.* 2024;16(2):e1957. doi:10.1002/wnan.1957
33. Cheng J, Yan J, Liu Y, et al. Cancer-cell-derived fumarate suppresses the anti-tumor capacity of CD8(+) T cells in the tumor microenvironment. *Cell Metab*. 2023;35(6):961–978.e10. doi:10.1016/j.cmet.2023.04.017
34. Zhu M, Liu Q, Chen Z, et al. Rational design of Dual-Targeted nanomedicines for enhanced vascular permeability in low-permeability tumors. *Acs Nano*. 2025;19(3):3424–3438. doi:10.1021/acsnano.4c12808
35. Yu H, Liu J, Bu X, et al. Targeting METTL3 reprograms the tumor microenvironment to improve cancer immunotherapy. *Cell Chem Biol*. 2024;31(4):776–791.e7. doi:10.1016/j.chembiol.2023.09.001
36. Li A, Zhang T, Zhang X, et al. Flexocatalytic reduction of tumor interstitial fluid/solid pressure for efficient nanodrug penetration. *ACS Nano*. 2024;18(7):5344–5357.
37. Ahmed Mohamed D. *PBPK Modelling for the Prediction of Iron Oxide Nanoparticle Systemic and Intratumoural Distribution in Prostate and Pancreatic Cancers–Towards Their Application in Hyperthermia Treatment*. University of Liverpool; 2024.
38. Wang H, Lan D, Cao H, et al. Self-propulsion of biomimetic nanomotors promotes diffusion and convection transport for enhanced radiotherapy in solid glioblastoma. *J Am Chem Soc*. 2025;147;(28):25072–87
39. Fan Q, Wu G, Chen M, et al. Cediranib ameliorates portal hypertensive syndrome via inhibition of VEGFR-2 signaling in cirrhotic rats. *Eur. J. Pharmacol*. 2024;964:176278. doi:10.1016/j.ejphar.2023.176278
40. Wang G, Zhou Z, Zhao Z, et al. Enzyme-triggered transcytosis of dendrimer–drug conjugate for deep penetration into pancreatic tumors. *ACS Nano*. 2020;14(4):4890–4904. doi:10.1021/acsnano.0c00974
41. Cahn D, Stern A, Buckenmeyer M, et al. Extracellular matrix limits nanoparticle diffusion and cellular uptake in a tissue-specific manner. *ACS Nano*. 2024;18(46):32045–32055. doi:10.1021/acsnano.4c10381
42. Begum HM, Oh JM, Kang DS, Yu M, Shen K. Physical regulations of cell interactions and metabolism in tumor microenvironments. In: *Engineering and Physical Approaches to Cancer*. Springer; 2023:139–157.
43. Guo KS, Brodsky AS. Tumor collagens predict genetic features and patient outcomes. *NPJ Genomic Med*. 2023;8(1):15. doi:10.1038/s41525-023-00358-9
44. Zhan M, Yu X, Zhao W, et al. Extracellular matrix-degrading STING nanoagonists for mild NIR-II photothermal-augmented chemodynamic-immunotherapy. *J Nanobiotechnol*. 2022;20(1):23. doi:10.1186/s12951-021-01226-3
45. Tseng K-Y, Stratoulias V, Hu W-F, et al. Augmenting hematoma-scavenging capacity of innate immune cells by CDNF reduces brain injury and promotes functional recovery after intracerebral hemorrhage. *Cell Death Dis*. 2023;14(2):128. doi:10.1038/s41419-022-05520-2
46. Yang X-Y, Zhang J-G, Zhou Q-M, et al. Extracellular matrix modulating enzyme functionalized biomimetic Au nanoplatform-mediated enhanced tumor penetration and synergistic antitumor therapy for pancreatic cancer. *J Nanobiotechnol*. 2022;20(1):524. doi:10.1186/s12951-022-01738-6
47. Wang R, Cheng L, He L, et al. Nitric oxide nano-reactor DNMF/PLGA enables tumor vascular microenvironment and chemo-hyperthermia synergetic therapy. *J Nanobiotechnol*. 2024;22(1):110. doi:10.1186/s12951-024-02366-y

48. Hodrea J, Tran MN, Besztercei B, et al. Sigma-1 receptor agonist fluvoxamine ameliorates fibrotic response of trabecular meshwork cells. *Int J Mol Sci*. 2023;24(14):11646. doi:10.3390/ijms241411646
49. Yong DX, Song AY, Mu L, et al. Potential function of MMP3 gene in degradation of extracellular matrix complex in colorectal carcinoma. *Biomed. Environ. Sci*. 2021;34(1):66–70. doi:10.3967/bes2021.009
50. Wan MM, Chen H, Da Wang Z, et al. Nitric oxide-driven nanomotor for deep tissue penetration and multidrug resistance reversal in cancer therapy. *Adv. Sci*. 2021;8(3):2002525. doi:10.1002/advs.202002525
51. Chen H, Shi T, Wang Y, et al. Deep penetration of nanolevel drugs and micrometer-level t cells promoted by nanomotors for cancer immunochemotherapy. *J Am Chem Soc*. 2021;143(31):12025–12037. doi:10.1021/jacs.1c03071
52. Khokhlova TD, Wang Y-N, Son H, et al. Chronic effects of pulsed high intensity focused ultrasound aided delivery of gemcitabine in a mouse model of pancreatic cancer. *Ultrasonics*. 2023;132:106993. doi:10.1016/j.ultras.2023.106993
53. Namakshenas P, Mojra A. Efficient drug delivery to hypoxic tumors using thermosensitive liposomes with encapsulated anti-cancer drug under high intensity pulsed ultrasound. *Int. J. Mech. Sci*. 2023;237:107818. doi:10.1016/j.ijmecsci.2022.107818
54. Choi Y, Han H, Jeon S, et al. Deep tumor penetration of doxorubicin-loaded glycol chitosan nanoparticles using high-intensity focused ultrasound. *Pharmaceutics*. 2020;12(10):974. doi:10.3390/pharmaceutics12100974
55. Soleymani M, Velashjerdi M, Asgari M. Preparation of hyaluronic acid-decorated mixed nanomicelles for targeted delivery of hydrophobic drugs to CD44-overexpressing cancer cells. *Int J Pharm*. 2021;592:120052. doi:10.1016/j.ijpharm.2020.120052
56. Jiang Z, Gu Y. Hyaluronidase induces degenerative effects on intervertebral endplate cells via upregulation of PTGS2. *Cytotechnology*. 2025;77(3):104. doi:10.1007/s10616-025-00764-0
57. Lee WT, Lee J, Kim H, et al. Photoreactive-proton-generating hyaluronidase/albumin nanoparticles-loaded PEG-hydrogel enhances antitumor efficacy and disruption of the hyaluronic acid extracellular matrix in AsPC-1 tumors. *Mater Today Bio*. 2021;12:100164. doi:10.1016/j.mtbio.2021.100164
58. Yang C, Fu Y, Huang C, et al. Chlorin e6 and CRISPR-Cas9 dual-loading system with deep penetration for a synergistic tumoral photodynamic-immunotherapy. *Biomaterials*. 2020;255:120194. doi:10.1016/j.biomaterials.2020.120194
59. Berezina OV, Rykov SV, Schwarz WH, et al. Xanthan: enzymatic degradation and novel perspectives of applications. *Appl. Microbiol. Biotechnol*. 2024;108(1):227. doi:10.1007/s00253-024-13016-6
60. Wu D, Chen X, Zhou J, et al. A synergistic optical strategy for enhanced deep-tumor penetration and therapy in the second near-infrared window. *Mater Horizons*. 2020;7(11):2929–2935. doi:10.1039/D0MH00870B
61. Bhat S, Viswanathan P, Chandanala S, et al. Expansion and characterization of bone marrow derived human mesenchymal stromal cells in serum-free conditions. *Sci Rep*. 2021;11(1):3403. doi:10.1038/s41598-021-83088-1
62. Tavakoli S, Ghaderi jafarbeigloo HR, Shariati A, et al. Mesenchymal stromal cells; a new horizon in regenerative medicine. *J Cell Physiol*. 2020;235(12):9185–9210. doi:10.1002/jcp.29803
63. García-Bernal D, García-Arranz M, Yáñez RM, et al. The current status of mesenchymal stromal cells: controversies, unresolved issues and some promising solutions to improve their therapeutic efficacy. *Front Cell Develop Biol*. 2021;9:650664. doi:10.3389/fcell.2021.650664
64. Mhaidly R, Mechta-Grigoriou F. Role of cancer-associated fibroblast subpopulations in immune infiltration, as a new means of treatment in cancer. *Immunol Rev*. 2021;302(1):259–272. doi:10.1111/imr.12978
65. Zhao Y, Shen M, Wu L, et al. Stromal cells in the tumor microenvironment: accomplices of tumor progression? *Cell Death Dis*. 2023;14(9):587. doi:10.1038/s41419-023-06110-6
66. Antoon R, Overdevest N, Saleh AH, et al. Mesenchymal stromal cells as cancer promoters. *Oncogene*. 2024;43(49):3545–3555. doi:10.1038/s41388-024-03183-1
67. Li HJ, Du J-Z, Du X-J, et al. Stimuli-responsive clustered nanoparticles for improved tumor penetration and therapeutic efficacy. *Proc Natl Acad Sci U S A*. 2016;113(15):4164–4169. doi:10.1073/pnas.1522080113
68. Goenka A, Khan F, Verma B, et al. Tumor microenvironment signaling and therapeutics in cancer progression. *Cancer Commun*. 2023;43(5):525–561. doi:10.1002/cac2.12416
69. Li Y, Wang C, Huang T, et al. The role of cancer-associated fibroblasts in breast cancer metastasis. *Front Oncol*. 2023;13:1194835. doi:10.3389/fonc.2023.1194835
70. Liu J, Zhang J, Gao Y, et al. Barrier permeation and improved nanomedicine delivery in tumor microenvironments. *Cancer Lett*. 2023;562:216166. doi:10.1016/j.canlet.2023.216166
71. Liu Y, Ye Z, Yang W, et al. A triple enhanced permeable gold nanoraspberry designed for positive feedback interventional therapy. *J Control Release*. 2022;345:120–137. doi:10.1016/j.jconrel.2022.03.010
72. Zhang Z, Wang H, Tan T, et al. Rational design of nanoparticles with deep tumor penetration for effective treatment of tumor metastasis. *Adv. Funct. Mater*. 2018;28(40):1801840. doi:10.1002/adfm.201801840
73. Xu Z, Huang H, Xiong X, et al. *A near-infrared light-responsive extracellular vesicle as a* "Trojan horse" *for tumor deep penetration and imaging-guided therapy. Biomaterials*. 2021;269:120647. doi:10.1016/j.biomaterials.2020.120647
74. Lin X, Zhu R, Hong Z, et al. GSH-responsive radiosensitizers with deep penetration ability for multimodal imaging-guided synergistic radio-chemodynamic cancer therapy. *Adv. Funct. Mater*. 2021;31(24):2101278. doi:10.1002/adfm.202101278
75. Hou X, Zhong D, Li Y, et al. Facile fabrication of multi-pocket nanoparticles with stepwise size transition for promoting deep penetration and tumor targeting. *J Nanobiotechnol*. 2021;19:1–13. doi:10.1186/s12951-021-00854-z
76. Li Z, Gao Y, Li W, et al. Charge-reversal nanomedicines as a smart bullet for deep tumor penetration. *Smart Mater Med*. 2022;3:243–253. doi:10.1016/j.smaim.2022.01.008
77. Gómez-Escudero J, Berlana-Galán P, Guerra-Paes E, et al. Vascular disruption therapy as a new strategy for cancer treatment. *Int J Mol Sci*. 2025;26(20):10085. doi:10.3390/ijms262010085
78. Wojtukiewicz MZ, Mysliwiec M, Matuszewska E, et al. Heterogeneous expression of proangiogenic and coagulation proteins in gliomas of different histopathological grade. *Pathol Oncol Res*. 2021;27:605017. doi:10.3389/pore.2021.605017
79. Wu D, Xu S, Zhang X, et al. A near-infrared laser-triggered size-shrinkable nanosystem with in situ drug release for deep tumor penetration. *ACS Appl Mater Interfaces*. 2021;13(14):16036–16047. doi:10.1021/acsami.1c00022
80. Zhang M, Ma H, Wang X, et al. Polysaccharide-based nanocarriers for efficient transvascular drug delivery. *J Control Release*. 2023;354:167–187. doi:10.1016/j.jconrel.2022.12.051

81. Tong RT, Boucher Y, Kozin SV, et al. Vascular normalization by vascular endothelial growth factor receptor 2 blockade induces a pressure gradient across the vasculature and improves drug penetration in tumors. *Cancer Res*. 2004;64(11):3731–3736. doi:10.1158/0008-5472.CAN-04-0074
82. Lee J, Kim S-E, Moon D, et al. A multilayered blood vessel/tumor tissue chip to investigate T cell infiltration into solid tumor tissues. *Lab on a Chip*. 2021;21(11):2142–2152. doi:10.1039/D1LC00182E
83. Lv B, Wang Y, Ma D, et al. Immunotherapy: reshape the tumor immune microenvironment. *Front Immunol*. 2022;13. doi:10.3389/fimmu.2022.844142
84. Shihab I, Khalil BA, Elemam NM, et al. Understanding the role of innate immune cells and identifying genes in breast cancer microenvironment. *Cancers*. 2020;12(8):2226. doi:10.3390/cancers12082226
85. Ginefra P, Lorusso G, Vannini N. Innate immune cells and their contribution to t-cell-based immunotherapy. *Int J Mol Sci*. 2020;21(12):4441. doi:10.3390/ijms21124441
86. Lu Q, Kou D, Lou S, et al. Nanoparticles in tumor microenvironment remodeling and cancer immunotherapy. *J Hematol Oncol*. 2024;17(1):16.
87. Dang B-T, Pham K-Y, Nguyen A-H, et al. Engineering nanoparticles to modulate extracellular matrix and immune components of the tumor microenvironment in cancer immunotherapy. *Biomater Res*. 2025;29. doi:10.34133/bmr.0289
88. Hu C, Wang J, Gao X, et al. Pluronic-based nanoparticles for delivery of doxorubicin to the tumor microenvironment by binding to macrophages. *ACS Nano*. 2024;18(22):14441–14456. doi:10.1021/acsnano.4c01120
89. Luo P-K, Chang W-A, Peng S-Y, et al. Endogenous macrophages as "Trojan horses" for targeted oral delivery of mRNA-encoded cytokines in tumor microenvironment immunotherapy. *Biomaterials*. 2026;325:123620. doi:10.1016/j.biomaterials.2025.123620
90. Chen K-H, Nguyen N, Huang T-Y, et al. Macrophage-hitchhiked orally administered β-glucans-functionalized nanoparticles as "precision-guided stealth missiles" for targeted pancreatic cancer therapy. *Adv. Mater.* 2023;35(40):2304735. doi:10.1002/adma.202304735
91. Su Y, Gao J, Dong X, et al. Neutrophil-mediated delivery of nanocrystal drugs via photoinduced inflammation enhances cancer therapy. *ACS Nano*. 2023;17(16):15542–15555. doi:10.1021/acsnano.3c02013
92. Wu J, Ma T, Zhu M, et al. A pluripotential neutrophil-mimic nanovehicle modulates immune microenvironment with targeted drug delivery for augmented antitumor chemotherapy. *ACS Nano*. 2024;18(7):5864–5877.
93. Chang Y, Cai X, Syahirah R, et al. CAR-neutrophil mediated delivery of tumor-microenvironment responsive nanodrugs for glioblastoma chemo-immunotherapy. *Nat Commun*. 2023;14(1):2266. doi:10.1038/s41467-023-37872-4
94. Zhang R, Jin T, Ren Y, et al. Harnessing nanotheranostics-based dendritic cells tracking mature tertiary lymphoid structures to boost anti-glioma immunotherapy. *Adv. Funct. Mater.* 2025;35(34):2425894. doi:10.1002/adfm.202425894
95. Ma X, Kuang L, Yin Y, et al. Tumor–antigen activated dendritic cell membrane-coated biomimetic nanoparticles with orchestrating immune responses promote therapeutic efficacy against glioma. *ACS Nano*. 2023;17(3):2341–2355. doi:10.1021/acsnano.2c09033
96. Yang S, et al. Advances in engineered macrophages: a new frontier in cancer immunotherapy. *Cell Death Dis*. 2024;15(4):238.
97. Yunna C, Mengru H, Lei W, et al. Macrophage M1/M2 polarization. *Eur. J. Pharmacol*. 2020;877:173090. doi:10.1016/j.ejphar.2020.173090
98. Anderson NR, Minutolo NG, Gill S, et al. Macrophage-based approaches for cancer immunotherapy. *Cancer Res*. 2021;81(5):1201–1208. doi:10.1158/0008-5472.CAN-20-2990
99. Gunassekaran GR, Poongkavithai Vadevoo SM, Baek M-C, et al. M1 macrophage exosomes engineered to foster M1 polarization and target the IL-4 receptor inhibit tumor growth by reprogramming tumor-associated macrophages into M1-like macrophages. *Biomaterials*. 2021;278:121137. doi:10.1016/j.biomaterials.2021.121137
100. Chen S, Saeed AFUH, Liu Q, et al. Macrophages in immunoregulation and therapeutics. *Signal Transduct Target Ther*. 2023;8(1):207. doi:10.1038/s41392-023-01452-1
101. Xu L, Miao J, Xu D, et al. Macrophage-targeted polysaccharide nano-immunomodulators with spatial- and time-programmed drug release for cancer therapy. *Nano Today*. 2026;66:102893. doi:10.1016/j.nantod.2025.102893
102. Hu Y, Nie W, Lyu L, et al. Tumor-microenvironment-activatable nanoparticle mediating immunogene therapy and M2 macrophage-targeted inhibitor for synergistic cancer immunotherapy. *ACS Nano*. 2024;18(4):3295–3312. doi:10.1021/acsnano.3c10037
103. Jiang N, Zhao K, Liu C, et al. Tumor microenvironment responsive multifunctional smart living materials based on engineered bacteria for inducing macrophage polarization to enhance tumor immunotherapy. *Chem Eng J*. 2024;488:150820. doi:10.1016/j.cej.2024.150820
104. Hiam-Galvez KJ, Allen BM, Spitzer MH. Systemic immunity in cancer. *Nat Rev Cancer*. 2021;21(6):345–359. doi:10.1038/s41568-021-00347-z
105. McKenna E, Mhaonaigh AU, Wubben R, et al. Neutrophils: need for standardized nomenclature. *Front Immunol*. 2021;12. doi:10.3389/fimmu.2021.602963
106. Zhang J, Gu J, Wang X, et al. Engineering and targeting neutrophils for cancer therapy. *Adv. Mater.* 2024;36(19):2310318. doi:10.1002/adma.202310318
107. Li H, Li C, Fu C, et al. Innovative nanoparticle-based approaches for modulating neutrophil extracellular traps in diseases: from mechanisms to therapeutics. *J Nanobiotechnol*. 2025;23(1):88. doi:10.1186/s12951-025-03195-3
108. Hao J, Chen J, Wang M, et al. *Neutrophils, as* "Trojan horses", *participate in the delivery of therapeutical PLGA nanoparticles into a tumor based on the chemotactic effect*. *Drug Delivery*. 2020;27(1):1–14. doi:10.1080/10717544.2019.1701141
109. Ding J, Sui D, Liu M, et al. Sialic acid conjugate-modified liposomes enable tumor homing of epirubicin via neutrophil/monocyte infiltration for tumor therapy. *Acta Biomater*. 2021;134:702–715. doi:10.1016/j.actbio.2021.07.063
110. Hargadon KM. Tumor microenvironmental influences on dendritic cell and T cell function: a focus on clinically relevant immunologic and metabolic checkpoints. *Clin Translat Med*. 2020;10(1):374–411. doi:10.1002/ctm2.37
111. Prakash M, Cortez CD, Jayaraman A, et al. Innovative gene engineering and drug delivery systems for dendritic cells in cancer immunotherapy. *J Biomed Sci*. 2025;32(1):95. doi:10.1186/s12929-025-01191-1
112. Huang F, Zhang Q, Xiao J, et al. Cancer cell membrane-coated gambogic acid nanoparticles for effective anticancer vaccination by activating dendritic cells. *Int J Nanomed*. 2023;Volume 18:2261–2273. doi:10.2147/IJN.S408521
113. Zhang Y, Hou X, Du S, et al. Close the cancer–immunity cycle by integrating lipid nanoparticle–mRNA formulations and dendritic cell therapy. *Nature Nanotechnol*. 2023;18(11):1364–1374. doi:10.1038/s41565-023-01453-9
114. Wu D, Chen Q, Chen X, et al. The blood–brain barrier: structure, regulation and drug delivery. *Signal Transduct Target Ther*. 2023;8(1):217. doi:10.1038/s41392-023-01481-w

115. Mojarad-Jabali S, Roh K-H. Peptide-based inhibitors and nanoparticles: emerging therapeutics for Alzheimer's disease. *Int J Pharm*. 2025;669:125055. doi:10.1016/j.ijpharm.2024.125055
116. Susa F, Arpicco S, Pirri CF, et al. An overview on the physiopathology of the blood–brain barrier and the lipid-based nanocarriers for central nervous system delivery. *Pharmaceutics*. 2024;16(7):849. doi:10.3390/pharmaceutics16070849
117. Singh SA, Vellapandian C. Structure of the blood brain barrier and its role in the transporters for the movement of substrates across the barriers. *Current Drug Metabolism*. 2023;24(4):250–269. doi:10.2174/1389200224666230608110349
118. Manu DR, Slevin M, Barcutean L, et al. Astrocyte involvement in blood–brain barrier function: a critical update highlighting novel, complex, neurovascular interactions. *Int J Mol Sci*. 2023;24(24):17146. doi:10.3390/ijms242417146
119. Zhou X, Smith QR, Liu X. Brain penetrating peptides and peptide–drug conjugates to overcome the blood–brain barrier and target CNS diseases. *Wiley Interdiscip. Rev.* 2021;13(4):e1695. doi:10.1002/wnan.1695
120. Narsinh KH, Perez E, Haddad AF, et al. Strategies to improve drug delivery across the blood–brain barrier for glioblastoma. *Curr Neurol Neurosci Rep*. 2024;24(5):123–139. doi:10.1007/s11910-024-01338-x
121. Marcucci F, Corti A, Ferreri AJ. Breaching the blood–brain tumor barrier for tumor therapy. *Cancers*. 2021;13(10):2391. doi:10.3390/cancers13102391
122. Morris EK, Daignault-Mill S, Stehbens SJ, et al. Addressing blood-brain-tumor-barrier heterogeneity in pediatric brain tumors with innovative preclinical models. *Front Oncol*. 2023;13:1101522. doi:10.3389/fonc.2023.1101522
123. Wang Y, Huo Y, Zhao C, et al. Engineered exosomes with enhanced stability and delivery efficiency for glioblastoma therapy. *J Control Release*. 2024;368:170–183. doi:10.1016/j.jconrel.2024.02.015
124. Song LL, Tang YP, Qu YQ, et al. Exosomal delivery of rapamycin modulates blood-brain barrier penetration and VEGF axis in glioblastoma. *J Control Release*. 2025;381:113605. doi:10.1016/j.jconrel.2025.113605
125. Zheng Z, Chen J, Kang Y, et al. Dual-responsive nanoparticle system for enhanced blood-brain barrier crossing and glioblastoma penetration. *Biomaterials*. 2026;327:123730. doi:10.1016/j.biomaterials.2025.123730
126. Yu T, Wang K, Wang J, et al. M-MDSCs mediated trans-BBB drug delivery for suppression of glioblastoma recurrence post-standard treatment. *J Control Release*. 2024;369:199–214. doi:10.1016/j.jconrel.2024.03.043
127. Gu X, Liu J, Xiang H, et al. Fixed-point cleaved bioinspired nanosystem via promoting LAT1-mediated BBB penetration for spatiotemporal therapy in TMZ resistant glioblastoma. *Chem Eng J*. 2025;517:164470. doi:10.1016/j.cej.2025.164470
128. Liu R, An Y, Jia W, et al. Macrophage-mimic shape changeable nanomedicine retained in tumor for multimodal therapy of breast cancer. *J Control Release*. 2020;321:589–601. doi:10.1016/j.jconrel.2020.02.043
129. Jia W, Gong B, Chen J, et al. Dual-responsive shape-transformable charge-reversible nanoparticles combined with chemo-photodynamic-immunotherapy for the treatment of breast cancer and lung metastasis. *Adv. Funct. Mater.* 2024;34:2408581. doi:10.1002/adfm.202408581
130. Xu Z, Pan C, Yuan W. Light-enhanced hypoxia-responsive and azobenzene cleavage-triggered size-shrinkable micelles for synergistic photodynamic therapy and chemotherapy. *Biomater. Sci*. 2020;8(12):3348–3358. doi:10.1039/D0BM00328J
131. Glassman PM, Villa CH, Marcos-Contreras OA, et al. Targeted in vivo loading of red blood cells markedly prolongs nanocarrier circulation. *Bioconjugate Chem*. 2022;33(7):1286–1294. doi:10.1021/acs.bioconjchem.2c00196
132. Huang Y, Yu M, Zheng J. Charge barriers in the kidney elimination of engineered nanoparticles. *Proc Natl Acad Sci*. 2024;121(23):e2403131121. doi:10.1073/pnas.2403131121
133. Shinde VR, Revi N, Murugappan S, et al. Enhanced permeability and retention effect: a key facilitator for solid tumor targeting by nanoparticles. *Photodiagn Photodyn Ther*. 2022;39:102915. doi:10.1016/j.pdpdt.2022.102915
134. Gong Z, Zhou B, Liu X, et al. Enzyme-induced transformable peptide nanocarriers with enhanced drug permeability and retention to improve tumor nanotherapy efficacy. *ACS Appl. Mater. Interfaces*. 2021;13(47):55913–55927. doi:10.1021/acsami.1c17917
135. Chen W, Wang B, Liang S, et al. Renal clearance of graphene oxide: glomerular filtration or tubular secretion and selective kidney injury association with its lateral dimension. *J Nanobiotechnol*. 2023;21(1):51. doi:10.1186/s12951-023-01781-x
136. Jia W, Liu R, Wang Y, et al. Dual-responsive nanoparticles with transformable shape and reversible charge for amplified chemo-photodynamic therapy of breast cancer. *Acta Pharmaceutica Sinica B*. 2022;12(8):3354–3366. doi:10.1016/j.apsb.2022.03.010
137. Lu C, Li Z, Wu N, et al. Tumor microenvironment-tailored nanoplatform for companion diagnostic applications of precise cancer therapy. *Chem*. 2023;9(11):3185–3211. doi:10.1016/j.chempr.2023.06.011
138. Liu Q, Tian X, Gong K, et al. Size Switchable self-assembled iron oxide aggregations loaded with doxorubicin for deep penetration and enhanced chemotherapy of cancer. *ACS Appl. Bio Mater.* 2023;7(1):297–305. doi:10.1021/acsabm.3c00889
139. Sun M, Zhou M, Xiao Y, et al. Reversibly size-switchable polyion complex micelles for antiangiogenic cancer therapy. *Chin. Chem. Lett*. 2024;35(7):109110. doi:10.1016/j.cclet.2023.109110
140. Hao Q, Wang Z, Zhao W, et al. Dual-responsive polyprodrug nanoparticles with cascade-enhanced magnetic resonance signals for deep-penetration drug release in tumor therapy. *ACS Appl. Mater. Interfaces*. 2020;12(44):49489–49501. doi:10.1021/acsami.0c16110
141. Feng W, Zong M, Wan L, et al. pH/redox sequentially responsive nanoparticles with size shrinkage properties achieve deep tumor penetration and reversal of multidrug resistance. *Biomater. Sci*. 2020;8(17):4767–4778. doi:10.1039/D0BM00695E
142. Zhu Y, Song Y, Cao Z, et al. Magnetically actuated active deep tumor penetration of deformable large nanocarriers for enhanced cancer therapy. *Adv. Funct. Mater.* 2021;31(35):2103655. doi:10.1002/adfm.202103655
143. Xu W, Wang J, Jin L, et al. A tumor acidity-driven transformable polymeric nanoassembly with deep tumor penetration and membrane-anchoring capability for targeted photodynamic therapy. *Biomaterials*. 2021;276:121024. doi:10.1016/j.biomaterials.2021.121024
144. Xu J, Chen S, Yang J, et al. Hyaluronidase-trigger nanocarriers for targeted delivery of anti-liver cancer compound. *RSC Adv.* 2023;13(16):11160–11170. doi:10.1039/D3RA00693J
145. Yang L, Yang Y, Zhang J, et al. Sequential responsive nano-PROTACs for precise intracellular delivery and enhanced degradation efficacy in colorectal cancer therapy. *Signal Transduct Target Ther*. 2024;9(1):275. doi:10.1038/s41392-024-01983-1
146. Hashemi M, Ghadyani F, Hasani S, et al. Nanoliposomes for doxorubicin delivery: reversing drug resistance, stimuli-responsive carriers and clinical translation. *J Drug Delivery Sci Technol*. 2023;80:104112.
147. Ma J-B, Shen J-M, Yue T, et al. Size-shrinkable and protein kinase Cα-recognizable nanoparticles for deep tumor penetration and cellular internalization. *Eur. J. Pharm. Sci*. 2021;159:105693. doi:10.1016/j.ejps.2020.105693

148. Huang Y, Wu S, Li J, et al. Self-amplified pH/ROS dual-responsive co-delivery nano-system with chemo-photodynamic combination therapy in hepatic carcinoma treatment. *Int J Nanomed*. 2024;Volume 19:3737–3751. doi:10.2147/IJN.S453199
149. Yuan J, Chen Q, Zuo M, et al. Enhanced combination therapy through tumor microenvironment-activated cellular uptake and ROS-sensitive drug release using a dual-sensitive nanogel. *Biomater. Sci*. 2025;13(6):1554–1567. doi:10.1039/D4BM01377H
150. Hoang QT, Lee D, Choi DG, et al. Efficient and selective cancer therapy using pro-oxidant drug-loaded reactive oxygen species (ROS)-responsive polypeptide micelles. *J Ind Eng Chem*. 2021;95:101–108. doi:10.1016/j.jiec.2020.12.009
151. Shen S, Liu X, Jiang P, et al. Nanoscale micelles loaded with Fe 3 O 4 nanoparticles for deep-tissue penetration and ferroptosis/sonodynamic tumor therapy. *ACS Appl. Nano Mater*. 2022;5(12):17664–17672. doi:10.1021/acsanm.2c03539
152. Li Y, Chen M, Yao B, et al. Dual pH/ROS-responsive nanoplatform with deep tumor penetration and self-amplified drug release for enhancing tumor chemotherapeutic efficacy. *Small*. 2020;16(32):2002188. doi:10.1002/smll.202002188
153. Gao W, Bigham A, Ghomi M, et al. Micelle-engineered nanoplatforms for precision oncology. *Chem Eng J*. 2024;495:153438. doi:10.1016/j.cej.2024.153438
154. Wu J, Liu W, Tang S, et al. Light-responsive smart nanoliposomes: harnessing the azobenzene moiety for controlled drug release under near-infrared irradiation. *ACS Appl. Mater. Interfaces*. 2024;16(42):56850–56861. doi:10.1021/acsami.4c13549
155. Sun B, Liu J, Kim HJ, et al. Light-responsive smart nanocarriers for wirelessly controlled photodynamic therapy for prostate cancers. *Acta Biomater*. 2023;171:553–564. doi:10.1016/j.actbio.2023.09.031
156. Chu Y, Xu X-Q, Wang Y. Ultradeep photothermal therapy strategies. *J Phys Chem Lett*. 2022;13(41):9564–9572. doi:10.1021/acs.jpclett.2c02642
157. Zhou S, Wang H, Li R, et al. Multifunctional self-assembly with NIR light-activated cascade effect for improving local treatment on solid tumors. *ACS Appl. Mater. Interfaces*. 2022;14(12):14087–14096. doi:10.1021/acsami.2c00448
158. Zhang P, Xu X, Ma X. NIR aggregate-biohybrid systems for biomedical applications. In: *Aggregation-Induced Emission: Applications in Biosensing, Bioimaging and Biomedicine–Volume 2*. Walter de Gruyter GmbH; 2022:317.
159. Peng J, Chen F, Liu Y, et al. A light-driven dual-nanotransformer with deep tumor penetration for efficient chemo-immunotherapy. *Theranostics*. 2022;12(4):1756–1768. doi:10.7150/thno.68756
160. Entezari M, Yousef Abad GG, Sedghi B, et al. Gold nanostructure-mediated delivery of anticancer agents: biomedical applications, reversing drug resistance, and stimuli-responsive nanocarriers. *Environ. Res*. 2023;225:115673. doi:10.1016/j.envres.2023.115673
161. Cong C, Jiaxin B, Liu X, et al. *A homologous-targeting* "nanoconverter" *with variable size for deep tumor penetration and immunotherapy. J Mat Chem B*. 2021;9(9):2323–2333. doi:10.1039/D0TB02908D
162. Pan X, Li P, Bai L, et al. Biodegradable nanocomposite with dual cell-tissue penetration for deep tumor chemo-phototherapy. *Small*. 2020;16(22):e2000809. doi:10.1002/smll.202000809
163. Abou Khouzam R, Janji B, Thiery J, et al. Hypoxia as a potential inducer of immune tolerance, tumor plasticity and a driver of tumor mutational burden: impact on cancer immunotherapy. *Semin Cancer Biol*. 2023;97:104–123. doi:10.1016/j.semcancer.2023.11.008
164. Xia Y, Duan S, Han C, et al. Hypoxia-responsive nanomaterials for tumor imaging and therapy. *Front Oncol*. 2022;12. doi:10.3389/fonc.2022.1089446
165. Filipczak N, Joshi U, Attia SA, et al. Hypoxia-sensitive drug delivery to tumors. *J Control Release*. 2022;341:431–442. doi:10.1016/j.jconrel.2021.11.034
166. Zhang Y, Xing J, Jiang J, et al. Hypoxia-responsive nanoparticles for fluorescence diagnosis and therapy of cancer. *Theranostics*. 2025;15(4):1353–1375. doi:10.7150/thno.104190
167. Kuperkar K, Patel D, Atanase LI, et al. Amphiphilic block copolymers: their structures, and self-assembly to polymeric micelles and polymersomes as drug delivery vehicles. *Polymers*. 2022;14(21):4702. doi:10.3390/polym14214702
168. Liu R, Hu C, Yang Y, et al. Theranostic nanoparticles with tumor-specific enzyme-triggered size reduction and drug release to perform photothermal therapy for breast cancer treatment. *Acta Pharmaceutica Sinica B*. 2019;9(2):410–420. doi:10.1016/j.apsb.2018.09.001
169. Bang S, Park B, Park JC, et al. Exosome-inspired lipid nanoparticles for enhanced tissue penetration. *ACS Nano*. 2025;19(9):8882–8894. doi:10.1021/acsnano.4c16629
170. Sulttan S, Rohani S. Modeling and simulation of smart magnetic self-assembled nanomicelle trajectories in an internal thoracic artery flow for breast cancer therapy. *Drug Delivery Transl Res*. 2023;13(2):675–688. doi:10.1007/s13346-022-01234-2
171. Lu B, Wang J, Hendriks AJ, et al. Clearance of nanoparticles from blood: effects of hydrodynamic size and surface coatings. *Environ Sci Nano*. 2024;11(1):406–417. doi:10.1039/D3EN00812F
172. Song M, Dong S, An X, et al. Erythrocyte-biomimetic nanosystems to improve antitumor effects of paclitaxel on epithelial cancers. *J Control Release*. 2022;345:744–754. doi:10.1016/j.jconrel.2022.03.060
173. Oberländer J, Champanhac C, da Costa Marques R, et al. Temperature, concentration, and surface modification influence the cellular uptake and the protein Corona of polystyrene nanoparticles. *Acta Biomater*. 2022;148:271–278. doi:10.1016/j.actbio.2022.06.028
174. Budiarta M, Roy S, Katenkamp T, et al. Overcoming non-specific interactions for efficient encapsulation of doxorubicin in ferritin nanocages for targeted drug delivery. *Small*. 2023;19(21):e2205606. doi:10.1002/smll.202205606
175. Yao Y, Dai X, Tan Y, et al. deep drug penetration of nanodrug aggregates at tumor tissues by fast extracellular drug release. *Adv Healthc Mater*. 2021;10(3):e2001430. doi:10.1002/adhm.202001430
176. Zeng X, Wang Y, Huang Y-S, et al. Amphiphilic metallodrug assemblies with red-light-enhanced cellular internalization and tumor penetration for anticancer phototherapy. *Small*. 2022;18(52):e2205461. doi:10.1002/smll.202205461
177. Mohd-Zahid MH, Zulkifli SN, Che Abdullah CA, et al. Gold nanoparticles conjugated with anti-CD133 monoclonal antibody and 5-fluorouracil chemotherapeutic agent as nanocarriers for cancer cell targeting. *RSC Adv*. 2021;11(26):16131–16141. doi:10.1039/D1RA01093J
178. Li C, Yang S, Li R, et al. Dual-aptamer-targeted immunomagnetic nanoparticles to accurately explore the correlations between circulating tumor cells and gastric cancer. *ACS Appl. Mater. Interfaces*. 2022;14(6):7646–7658. doi:10.1021/acsami.1c22720
179. Ramesh A, Malik V, Ranjani HA, et al. Rational combination of an immune checkpoint inhibitor with CSF1R inhibitor–loaded nanoparticle enhances anticancer efficacy. *Drug Delivery Transl Res*. 2021;11(6):2317–2327. doi:10.1007/s13346-021-01040-2
180. Hsieh P-H, Huang W-Y, Wang H-C, et al. Dual-responsive polypeptide nanoparticles attenuate tumor-associated stromal desmoplasia and anticancer through programmable dissociation. *Biomaterials*. 2022;284:121469. doi:10.1016/j.biomaterials.2022.121469

181. Xu L, Xu M, Sun X, et al. Quantitative comparison of gold nanoparticle delivery via the Enhanced Permeation and Retention (EPR) Effect and Mesenchymal Stem Cell (MSC)-Based Targeting. *ACS Nano*. 2023;17(3):2039–2052. doi:10.1021/acsnano.2c07295
182. Li D, Yang Y, Zheng G, et al. The potential of cellular homing behavior in tumor immunotherapy: from basic discoveries to clinical applications of immune, mesenchymal stem, and cancer cell homing. *Front Immunol*. 2024;15:1495978. doi:10.3389/fimmu.2024.1495978
183. Jin Y, Wu Z, Wu C, et al. Size-adaptable and ligand (biotin)-sheddable nanocarriers equipped with avidin scavenging technology for deep tumor penetration and reduced toxicity. *J Control Release*. 2020;320:142–158. doi:10.1016/j.jconrel.2020.01.040
184. Andhari SS, Wavhale RD, Dhobale KD, et al. Self-propelling targeted magneto-nanobots for deep tumor penetration and ph-responsive intracellular drug delivery. *Sci Rep*. 2020;10(1):4703. doi:10.1038/s41598-020-61586-y
185. Xiong X, Xu Z, Huang H, et al. A NIR light triggered disintegratable nanoplatform for enhanced penetration and chemotherapy in deep tumor tissues. *Biomaterials*. 2020;245:119840. doi:10.1016/j.biomaterials.2020.119840
186. Yang M, Wang X, Pu F, et al. Engineered exosomes-based photothermal therapy with mri/ct imaging guidance enhances anticancer efficacy through deep tumor nucleus penetration. *Pharmaceutics*. 2021;13(10):1593. doi:10.3390/pharmaceutics13101593
187. Asha Krishnan M, Yadav K, Roach P, et al. A targeted near-infrared nanoprobe for deep-tissue penetration and imaging of prostate cancer. *Biomater. Sci*. 2021;9(6):2295–2312. doi:10.1039/D0BM01970D
188. Gupta R, Kaur T, Chauhan A, et al. Tailoring nanoparticles design for enhanced heating efficiency and improved magneto-chemo therapy for glioblastoma. *Biomater. Adv*. 2022;139:213021. doi:10.1016/j.bioadv.2022.213021
189. Pandey P, Patel JK, Kumar S. Nanoparticle properties affecting the drug release, absorption, and pharmacokinetics of nanoparticulate drug delivery systems. In: *Pharmacokinetics and Pharmacodynamics of Nanoparticulate Drug Delivery Systems*. Springer; 2022:25–40.
190. Wu J, Zhu Z, Liu W, et al. How nanoparticles open the paracellular route of biological barriers: mechanisms, applications, and prospects. *ACS Nano*. 2022;16(10):15627–15652. doi:10.1021/acsnano.2c05317
191. Chen J, Jiang Z, Zhang YS, et al. Smart transformable nanoparticles for enhanced tumor theranostics. *Appl. Phys. Rev*. 2021;8(4). doi:10.1063/5.0061530.
192. Hamilton S, Kingston BR. Applying artificial intelligence and computational modeling to nanomedicine. *Curr. Opin. Biotechnol*. 2024;85:103043. doi:10.1016/j.copbio.2023.103043
193. Singh AV, Ansari MHD, Rosenkranz D, et al. Artificial Intelligence and machine learning in computational nanotoxicology: unlocking and empowering nanomedicine. *Adv Healthc Mater*. 2020;9(17):e1901862. doi:10.1002/adhm.201901862
194. Jayasinghe MK, Lee CY, Tran TTT, et al. The role of in silico research in developing nanoparticle-based therapeutics. *Front. Digit. Health*. 2022;4.
195. Aumklad P, Suriyaamporn P, Panomsuk S, et al. Artificial intelligence-aided rational design and prediction model for progesterone-loaded self-microemulsifying drug delivery system formulations. *Science, Engineering and Health Studies*;2024. 24050002. doi:10.69598/sehs.18.24050002
196. Singh AV, Varma M, Laux P, et al. Artificial intelligence and machine learning disciplines with the potential to improve the nanotoxicology and nanomedicine fields: a comprehensive review. *Arch. Toxicol*. 2023;97(4):963–979. doi:10.1007/s00204-023-03471-x
197. Santo KP, Neimark AV. Dissipative particle dynamics simulations in colloid and Interface science: a review. *Adv. Colloid Interface Sci*. 2021;298:102545. doi:10.1016/j.cis.2021.102545
198. Lin Z, Chou W-C, Cheng Y-H, et al. Predicting nanoparticle delivery to tumors using machine learning and artificial intelligence approaches. *Int J Nanomed*. 2022;17:1365–1379.
199. Mahdi WA, Alhowyan A, Obaidullah AJ. Intelligence analysis of drug nanoparticles delivery efficiency to cancer tumor sites using machine learning models. *Sci Rep*. 2025;15(1):1017. doi:10.1038/s41598-024-84450-9
200. Zhu M, Zhuang J, Li Z, et al. Machine-learning-assisted single-vessel analysis of nanoparticle permeability in tumour vasculatures. *Nat Nanotechnol*. 2023;18(6):657–666. doi:10.1038/s41565-023-01323-4
201. Ortiz-Perez A, van Tilborg D, van der Meel R, et al. Machine learning-guided high throughput nanoparticle design. *Digital Discovery*. 2024;3(7):1280–1291. doi:10.1039/D4DD00104D
202. Chen Q, Yuan L, Chou W-C, et al. Meta-analysis of nanoparticle distribution in tumors and major organs in tumor-bearing mice. *ACS Nano*. 2023;17(20):19810–19831. doi:10.1021/acsnano.3c04037
203. Maharjan R, Hada S, Lee JE, et al. Comparative study of lipid nanoparticle-based mRNA vaccine bioprocess with machine learning and combinatorial artificial neural network-design of experiment approach. *Int J Pharm*. 2023;640:123012. doi:10.1016/j.ijpharm.2023.123012
204. Kapoor DU, Sharma JB, Gandhi SM, et al. AI-driven design and optimization of nanoparticle-based drug delivery systems. *Science, Engineering and Health Studies*;2024. 24010003. doi:10.69598/sehs.18.24010003
205. Liu S, Zhang Y, Cui Y, et al. Enhancing drug-drug interaction prediction using deep attention neural networks. *IEEE/ACM transactions on Computational Biology and Bioinformatics*. 2022;20(2):976–985. doi:10.1109/TCBB.2022.3172421
206. Vitacolonna M, Bruch R, Schneider R, et al. A spheroid whole mount drug testing pipeline with machine-learning based image analysis identifies cell-type specific differences in drug efficacy on a single-cell level. *BMC Cancer*. 2024;24(1):1542. doi:10.1186/s12885-024-13329-9
207. Ngo TKN, Yang SJ, Mao B-H, et al. A deep learning-based pipeline for analyzing the influences of interfacial mechanochemical microenvironments on spheroid invasion using differential interference contrast microscopic images. *Mater Today Bio*. 2023;23:100820. doi:10.1016/j.mtbio.2023.100820
208. Nikfarjam Z, Zargari F. Advancements in deep learning for predicting drug-lipid interactions in liposomal drug delivery. *Arch. Comput. Methods Eng*. 2025;1–27.
209. Dai M, Demirel MF, Liang Y, et al. Graph neural networks for an accurate and interpretable prediction of the properties of polycrystalline materials. *NPJ Comput Mater*. 2021;7(1):103. doi:10.1038/s41524-021-00574-w
210. Hamzic S, Lewis R, Desrayaud S, et al. Predicting in vivo compound brain penetration using multi-task graph neural networks. *J Chem Inf Model*. 2022;62(13):3180–3190. doi:10.1021/acs.jcim.2c00412
211. Xia X, Sivonxay E, Helms BA, et al. Accelerating the design of multishell upconverting nanoparticles through Bayesian optimization. *Nano Lett*. 2023;23(23):11129–11136. doi:10.1021/acs.nanolett.3c03568
212. Sano S, Kadowaki T, Tsuda K, et al. Application of Bayesian optimization for pharmaceutical product development. *J Pharm Innovation*. 2020;15(3):333–343. doi:10.1007/s12247-019-09382-8

213. Wang F, Parhizkar M, Harker A, et al. Constrained composite Bayesian optimization for rational synthesis of polymeric particles. *Digital Discovery*. 2025;4(11):3066–3077. doi:10.1039/D5DD00243E
214. Bhujel R, Enkmann V, Burgstaller H, et al. Artificial intelligence-driven strategies for targeted delivery and enhanced stability of RNA-based lipid nanoparticle cancer vaccines. *Pharmaceutics*. 2025;17(8):992. doi:10.3390/pharmaceutics17080992
215. Molla G, Bitew M. Revolutionizing personalized medicine: synergy with multi-omics data generation, main hurdles, and future perspectives. *Biomedicines*. 2024;12(12):2750. doi:10.3390/biomedicines12122750
216. Wang Y, Xiao Z, Wang Z, et al. Multi-omics approaches to decipher the interactions of nanoparticles and biological systems. *Nat. Rev. Bioeng*. 2025;3(4):333–348. doi:10.1038/s44222-024-00264-4
217. Haider M, Jagal J, Bajbouj K, et al. Integrated multi-omics analysis reveals unique signatures of paclitaxel-loaded poly(lactide- co -glycolide) nanoparticles treatment of head and neck cancer cells. *Proteomics*. 2023;23(16):2200380. doi:10.1002/pmic.202200380
218. Ruan C, Wang C, Gong X, et al. An integrative multi-omics approach uncovers the regulatory role of CDK7 and CDK4 in autophagy activation induced by silica nanoparticles. *Autophagy*. 2021;17(6):1426–1447. doi:10.1080/15548627.2020.1763019
219. Zhang Z, Chen F, Fang J, et al. Metal and non-metal nanoparticles differentially regulate flavonoid accumulation in Cyclocarya paliurus: a multi-omics analysis. *Ind Crops Prod*. 2025;236:122023. doi:10.1016/j.indcrop.2025.122023
220. Baysoy A, Bai Z, Satija R, et al. The technological landscape and applications of single-cell multi-omics. *Nat Rev Mol Cell Biol*. 2023;24(10):695–713. doi:10.1038/s41580-023-00615-w
221. Cao Z-J, Gao G. Multi-omics single-cell data integration and regulatory inference with graph-linked embedding. *Nature Biotechnol*. 2022;40(10):1458–1466. doi:10.1038/s41587-022-01284-4
222. Wen H, Ding J, Jin W, Wang Y, Xie Y, Tang J. Graph neural networks for multimodal single-cell data integration. In: *Proceedings of the 28th ACM SIGKDD conference on knowledge discovery and data mining*. 2022.
223. Wang C, Lue W, Kaalia R, et al. Network-based integration of multi-omics data for clinical outcome prediction in neuroblastoma. *Sci Rep*. 2022;12(1):15425. doi:10.1038/s41598-022-19019-5
224. Singhal A, Sevink GJ. The role of size and nature in nanoparticle binding to a model lung membrane: an atomistic study. *Nanoscale Adv*. 2021;3(23):6635–6648. doi:10.1039/D1NA00578B
225. Okoampah E, Mao Y, Yang S, et al. Gold nanoparticles-biomembrane interactions: from fundamental to simulation. *Colloids Surf B Biointerfaces*. 2020;196:111312. doi:10.1016/j.colsurfb.2020.111312
226. Huang-Zhu CA, Sheavly JK, Chew AK, et al. Ligand lipophilicity determines molecular mechanisms of nanoparticle adsorption to lipid bilayers. *ACS Nano*. 2024;18(8):6424–6437. doi:10.1021/acsnano.3c11854
227. Wang J, Han Y, Xu Z, et al. Dissipative particle dynamics simulation: a review on investigating mesoscale properties of polymer systems. *Macromol Mater Eng*. 2021;306(4):2000724. doi:10.1002/mame.202000724
228. Donadoni E, Siani P, Frigerio G, et al. The effect of polymer coating on nanoparticles' interaction with lipid membranes studied by coarse-grained molecular dynamics simulations. *Nanoscale*. 2024;16(18):9108–9122. doi:10.1039/D4NR00495G
229. Baiao A, Dias S, Soares AF, et al. Advances in the use of 3D colorectal cancer models for novel drug discovery. *Expert Opin Drug Discov*. 2022;17(6):569–580. doi:10.1080/17460441.2022.2056162
230. Jubelin C, Muñoz-Garcia J, Griscom L, et al. Three-dimensional in vitro culture models in oncology research. *Cell Biosci*. 2022;12(1):155. doi:10.1186/s13578-022-00887-3
231. Urzì O, Gasparro R, Costanzo E, et al. Three-dimensional cell cultures: the bridge between in vitro and in vivo models. *Int J Mol Sci*. 2023;24(15):12046. doi:10.3390/ijms241512046
232. Soeiro JF, Sousa FL, Monteiro MV, et al. Advances in screening hyperthermic nanomedicines in 3D tumor models. *Nanoscale Horiz*. 2024;9(3):334–364. doi:10.1039/D3NH00305A
233. Barbosa MA, Xavier CPR, Pereira RF, et al. 3D cell culture models as recapitulators of the tumor microenvironment for the screening of anti-cancer drugs. *Cancers*. 2021;14(1):190. doi:10.3390/cancers14010190
234. Roma-Rodrigues C, Pombo I, Fernandes AR, et al. Hyperthermia induced by gold nanoparticles and visible light photothermy combined with chemotherapy to tackle doxorubicin sensitive and resistant colorectal tumor 3D spheroids. *Int J Mol Sci*. 2020;21(21):8017. doi:10.3390/ijms21218017
235. Alves SR, Calori IR, Bi H, et al. Characterization of glioblastoma spheroid models for drug screening and phototherapy assays. *OpenNano*. 2023;9:100116. doi:10.1016/j.onano.2022.100116
236. Kirsh SM, Pascetta SA, Uniacke J. Spheroids as a 3D model of the hypoxic tumor microenvironment. In: *The Tumor Microenvironment: Methods and Protocols*. Springer; 2023:273–285.
237. Yuan X, Wang S, Yuan Z, et al. Boosting the angiogenesis potential of self-assembled mesenchymal stem cell spheroids by size mediated physiological hypoxia for vascularized pulp regeneration. *Acta Biomater*. 2025;198:102–114. doi:10.1016/j.actbio.2025.04.019
238. Vakhshiteh F, Bagheri Z, Soleimani M, et al. Heterotypic tumor spheroids: a platform for nanomedicine evaluation. *J Nanobiotechnol*. 2023;21(1):249. doi:10.1186/s12951-023-02021-y
239. Rani M, Devi A, Singh SP, Kumari R, Kumar A. 3D Cell Culture Techniques. In: *Animal Cell Culture: Principles and Practice*. Springer; 2023:197–212.
240. Mitrakas AG, Tsolou A, Didaskalou S, et al. Applications and advances of multicellular tumor spheroids: challenges in their development and analysis. *Int J Mol Sci*. 2023;24(8):6949. doi:10.3390/ijms24086949
241. Han SJ, Kwon S, Kim KS. Challenges of applying multicellular tumor spheroids in preclinical phase. *Can Cell Inter*. 2021;21(1):152. doi:10.1186/s12935-021-01853-8
242. Gunti S, Hoke ATK, Vu KP, et al. Organoid and spheroid tumor models: techniques and applications. *Cancers*. 2021;13(4):874. doi:10.3390/cancers13040874
243. Świerczewska M, Sterzyńska K, Ruciński M, et al. The response and resistance to drugs in ovarian cancer cell lines in 2D monolayers and 3D spheroids. *Biomed. Pharmacother*. 2023;165:115152. doi:10.1016/j.biopha.2023.115152
244. Pinto B, Henriques AC, Silva PMA, et al. Three-dimensional spheroids as in vitro preclinical models for cancer research. *Pharmaceutics*. 2020;12(12):1186. doi:10.3390/pharmaceutics12121186

245. Pratiwi FW, Peng -C-C, Wu S-H, et al. Evaluation of nanoparticle penetration in the tumor spheroid using two-photon microscopy. *Biomedicines*. 2021;9(1):10. doi:10.3390/biomedicines9010010
246. Nagesetti A, Dulikravich GS, Orlande HRB, et al. Computational model of silica nanoparticle penetration into tumor spheroids: effects of methoxy and carboxy PEG surface functionalization and hyperthermia. *Int. J. Numer. Methods Biomed. Eng*. 2021;37(8):e3504. doi:10.1002/cnm.3504
247. Ahmed-Cox A, Pandzic E, Johnston ST, et al. Spatio-temporal analysis of nanoparticles in live tumor spheroids impacted by cell origin and density. *J Control Release*. 2022;341:661–675. doi:10.1016/j.jconrel.2021.12.014
248. Zhou B, Feng Z, Xu J, et al. Organoids: approaches and utility in cancer research. *Chin Med J*. 2023;136(15):1783–1793. doi:10.1097/CM9.0000000000002477
249. Chen L, Luo X, Zhang J, et al. Harnessing organoid platforms for nanoparticle drug development. *Drug Des Devel Ther*. 2025; Volume 19:6125–6143. doi:10.2147/DDDT.S530999
250. Baek A, Kwon IH, Lee D-H, et al. Novel organoid culture system for improved safety assessment of nanomaterials. *Nano Lett*. 2024;24(3):805–813. doi:10.1021/acs.nanolett.3c02939
251. Schutgens F, Clevers H. Human organoids: tools for understanding biology and treating diseases. *Annu. Rev. Pathol*. 2020;15:211–234.
252. Gasco S, Muñoz-Fernández MÁ. A review on the current knowledge on zikv infection and the interest of organoids and nanotechnology on development of effective therapies against zika infection. *Int J Mol Sci*. 2021;22(1):35. doi:10.3390/ijms22010035
253. Rauth S, Karmakar S, Batra SK, et al. Recent advances in organoid development and applications in disease modeling. *Biochimica Et Biophysica Acta (BBA)-Reviews on Cancer*. 2021;1875(2):188527. doi:10.1016/j.bbcan.2021.188527
254. Shankaran A, Prasad K, Chaudhari S, et al. Advances in development and application of human organoids. *3 Biotech*. 2021;11(6):257. doi:10.1007/s13205-021-02815-7
255. Andrews MG, Kriegstein AR. Challenges of organoid research. *Annu. Rev. Neurosci*. 2022;45(1):23–39. doi:10.1146/annurev-neuro-111020-090812
256. Spiller ER, Ung N, Kim S, et al. Imaging-based machine learning analysis of patient-derived tumor organoid drug response. *Front Oncol*. 2021;11. doi:10.3389/fonc.2021.771173
257. Ferreira N, Kulkarni A, Agorku D, et al. OrganoIDNet: a deep learning tool for identification of therapeutic effects in PDAC organoid-PBMC co-cultures from time-resolved imaging data. *Cell Oncol*. 2025;48(1):101–122. doi:10.1007/s13402-024-00958-2
258. Foglizzo V, Cocco E, Marchiò S. Advanced cellular models for preclinical drug testing: from 2D cultures to organ-on-a-chip technology. *Cancers*. 2022;14(15):3692. doi:10.3390/cancers14153692
259. Moysidou C-M, Barberio C, Owens RM. Advances in engineering human tissue models. *Front Bioeng Biotechnol*. 2021;8:620962. doi:10.3389/fbioe.2020.620962
260. Li B, Tang Y, Huang Z, et al. Synergistic innovation in organ-on-a-chip and organoid technologies: reshaping the future of disease modeling, drug development, and precision medicine. *Protein and Cell*;2025. pwaf058. doi:10.1093/procel/pwaf058
261. Cao UMN, Zhang Y, Chen J, et al. Microfluidic Organ-on-A-chip: a Guide to Biomaterial Choice and Fabrication. *Int J Mol Sci*. 2023;24(4):3232. doi:10.3390/ijms24043232
262. Sontheimer-Phelps A, Hassell BA, Ingber DE. Modelling cancer in microfluidic human organs-on-chips. *Nat Rev Cancer*. 2019;19(2):65–81. doi:10.1038/s41568-018-0104-6
263. Leung CM, De Haan P, Ronaldson-Bouchard K, et al. A guide to the organ-on-a-chip. *Nat Rev Method Primers*. 2022;2(1):33.
264. Low LA, Mummery C, Berridge BR, et al. Organs-on-chips: into the next decade. *Nat Rev Drug Discov*. 2021;20(5):345–361. doi:10.1038/s41573-020-0079-3
265. Hargrove-Grimes P, Low LA, Tagle DA. Microphysiological systems: stakeholder challenges to adoption in drug development. *Cells Tissues Organs*. 2022;211(3):269–281. doi:10.1159/000517422
266. Regmi S, Poudel C, Adhikari R, et al. Applications of microfluidics and organ-on-a-chip in cancer research. *Biosensors*. 2022;12(7):459. doi:10.3390/bios12070459
267. Wang Y, Gao Y, Pan Y, et al. Emerging trends in organ-on-a-chip systems for drug screening. *Acta Pharmaceutica Sinica B*. 2023;13(6):2483–2509. doi:10.1016/j.apsb.2023.02.006
268. Liu X, Fang J, Huang S, et al. Tumor-on-a-chip: from bioinspired design to biomedical application. *Microsys Nanoeng*. 2021;7(1):50. doi:10.1038/s41378-021-00277-8
269. Yu Y, Zhou T, Cao L. Use and application of organ-on-a-chip platforms in cancer research. *J Cell Commun Signal*. 2023;17(4):1163–1179. doi:10.1007/s12079-023-00790-7
270. Xu H, Wen J, Yang J, et al. Tumor-microenvironment-on-a-chip: the construction and application. *Cell Commun Signaling*. 2024;22(1):515. doi:10.1186/s12964-024-01884-4
271. Li C, Holman JB, Shi Z, et al. On-chip modeling of tumor evolution: advances, challenges and opportunities. *Mater Today Bio*. 2023;21:100724. doi:10.1016/j.mtbio.2023.100724
272. Johnson A, Reimer S, Childres R, et al. The applications and challenges of the development of in vitro tumor microenvironment chips. *Cell. Mol. Bioeng*. 2023;16(1):3–21. doi:10.1007/s12195-022-00755-7
273. Das R, Fernandez JG. Biomaterials for mimicking and modelling tumor microenvironment. In: *Microfluidics and Biosensors in Cancer Research: Applications in Cancer Modeling and Theranostics*. Springer; 2022:139–170.
274. Oh JM, Park Y, Lee J, et al. Microfabricated organ-specific models of tumor microenvironments. *Annu. Rev. Biomed. Eng*. 2025;27(1):307–333. doi:10.1146/annurev-bioeng-110222-103522
275. Guo QR, Zhang -L-L, Liu J-F, et al. Multifunctional microfluidic chip for cancer diagnosis and treatment. *Nanotheranostics*. 2021;5(1):73–89. doi:10.7150/ntno.49614
276. Moerdler B, Krasner M, Orenbuch E, et al. PTOLEMI: personalized cancer treatment through machine learning-enabled image analysis of microfluidic assays. *Diagnostics*. 2023;13(19):3075. doi:10.3390/diagnostics13193075
277. Chiang -C-C, Anne R, Chawla P, et al. Deep learning unlocks label-free viability assessment of cancer spheroids in microfluidics. *Lab on a Chip*. 2024;24(12):3169–3182. doi:10.1039/D4LC00197D
278. Deng L, Olea AR, Ortiz-Perez A, et al. imaging diffusion and stability of single-chain polymeric nanoparticles in a multi-gel tumor-on-a-chip microfluidic device. *Small Methods*. 2024;8(10):2301072. doi:10.1002/smtd.202301072